

Spectra of glueballs and oddballs and the equation of state from holographic QCD

Lin Zhang,^a Chutian Chen,^b Yidian Chen^a and Mei Huang^a

^a*School of Nuclear Science and Technology, University of Chinese Academy of Sciences, Beijing, P.R.China 100049*

^b*School of Physical Sciences, University of Chinese Academy of Sciences, Beijing, P.R.China 100049*

E-mail: zhanglin@ucas.ac.cn, chenchutian18@mails.ucas.ac.cn,
chenyidian@ucas.ac.cn, huangmei@ucas.ac.cn

ABSTRACT: We study the spectra of two-gluon glueballs and three-gluon oddballs and corresponding equation of state in 5-dimensional deformed holographic QCD models in the graviton-dilaton system, where the metric, the dilaton field and dilaton potential are self-consistently solved from each other through the Einstein field equations and the equation of motion of the dilaton field. We compare the models by inputting the dilaton field, inputting the deformed metric and inputting the dilaton potential, and find that with only 2 parameters, the 5-dimensional holographic QCD model predictions on glueballs/oddballs spectra in general are in good agreement with lattice results except two oddballs 0^{+-} and 2^{+-} . From the results of glueballs/oddballs spectra at zero temperature and the equation of state at finite temperature, we observe that the model with quadratic dilaton field can simultaneously describe glueballs/oddballs spectra as well as equation of state of pure gluon system. The model with quadratic $A_E(z)$ can describe glueballs/oddballs spectra, but its corresponding equation of state behaves more like $N_f = 2 + 1$ quark matter. These are consistent with dimension analysis at UV boundary.

KEYWORDS: Glueballs, Oddballs, Equation of state, Holographic QCD

Contents

1	Introduction	2
2	The general Einstein-Maxwell-dilaton system	4
2.1	The Einstein-Maxwell-dilaton system in the Einstein frame	4
3	Five different models in the EMD system	6
3.1	Vacuum solutions: set I	7
3.2	Vacuum solutions: set II	8
3.3	Five different models	9
3.3.1	Model I and II	10
3.3.2	Model III and IV	12
3.3.3	Model V	13
4	Spectra of glueballs and oddballs	14
4.1	Glueballs and oddballs	15
4.2	Equation of motion for scalar, vector and tensor glueballs/oddballs	16
4.3	Numerical results of glueballs/oddballs spectra	18
4.3.1	Model I and II	18
4.3.2	Model III and IV	18
4.3.3	Model V	19
4.3.4	Compare results with lattice QCD, QCD sum rule and pp high energy scattering	19
5	Equation of state	23
5.1	Model I and II	23
5.2	Model III and IV	25
5.3	Model V	27
6	Conclusion and discussion	28

1 Introduction

Glueball is one of the most crucial predictions from quantum chromodynamics (QCD), whose non-Abelian feature makes it possible to form bound states of gauge bosons, i.e. glueballs made of two/three gluons (gg, ggg, etc.) [1]. The gauge field plays a more important dynamical role in glueballs than that in the standard hadrons, therefore studying particles like glueballs offers a good opportunity of understanding non-perturbative aspects of QCD. The glueball spectra has attracted much attention for four decades [1], and it has been widely investigated by using various non-perturbative methods. For example, glueballs have been studied by using lattice QCD [2–11], by using effective models like flux tube model [12] and MIT bag model [13–17], by using QCD sum rules [18–32] as well as by using relativistic many-body approach [33–35]. There are also some other analyses of glueballs in Refs. [36–44]. For more information, please refer to review papers [45–47].

On the other hand, the spin and mass of the glueball can be constrained from high energy scattering data. Regge trajectories $\alpha(t) = \alpha_0 + \alpha' t$ of the glueball have been used to fit high energy pp and $p\bar{p}$ scattering cross-section. The C-even glueball, Pomeron exchange gives the lightest $J = 2^{++}$ glueball mass $M = \sqrt{t} = 1.92 \text{ GeV}$. Analogy with the "Pomeron", C parity odd "Odderon" contributing to large odd amplitude was proposed in 1970s in describing the high energy pp and $p\bar{p}$ scattering [48, 49]. The Odderon was regarded as three-gluon state:

$$O_{abc}^{\mu\nu\sigma}(k1, k2, k3) = d_{abc} G_a^\mu(k1) G_b^\nu(k2) G_c^\sigma(k3) \quad (1.1)$$

where the lower indices refer to color and the upper ones refer to the Lorentz structure, and d_{abc} is the fundamental symmetric tensor in SU(3). The evidence for the identification of the odderon has been debated for a longtime. Recently, the D0 and TOTEM Collaborations announced the evidence of a t-channel exchanged C-odd odderons in pp and $p\bar{p}$ scattering [50, 51]. Especially the odderon's contribution at the dip-bump region is very essential. The mass of 3^{--} odderon $M_{3^{--}} = 3.001 \text{ GeV}$ and decay width $\Gamma_{3^{--}} = 2.984 \text{ GeV}$ are extracted by using the dipole (DP) Regge model to fit the scattering data [52–55].

In Ref. [32], the oddball spectra has been calculated by using the QCD sum rule. In this work, we are going to investigate the glueball spectra in the framework of holographic QCD, which is based on the gravity/gauge duality, or anti-de Sitter/conformal field theory (AdS/CFT) correspondence [56–58]. AdS/CFT correspondence offers a new possibility to tackle the difficulty of strongly coupled gauge theories [59–62]. Many efforts from both top-down and bottom-up approaches have been paid on examining the non-perturbative properties of QCD [63], e.g., QCD equation of state, phase transitions, fluid properties of quark-gluon plasma, meson spectra [64–75], baryon spectra [76–78], as well as the glueball sector [79–99]. In Refs. [100, 101], by linearizing the fluctuations around a classical σ -model coupled to gravity in $d + 1$ dimensions, a gauge invariant (diffeomorphism invariant) formalism for calculating the spectra of scalar glueballs and tensor glueballs was developed, which was initially proposed in Refs. [102–104]. This algorithmic formalism was tested and some non-trivial applications were given in Refs. [105–114]. The glueball mass spectra and decay rate in the Sakai-Sugimoto model have been investigated in Refs. [115–117]. Glueballs

and oddballs spectra have also been widely studied by using the bottom-up approach, where some studies are based on hard-wall [64] and soft-wall holographic QCD models [65] with the conformal AdS_5 background metric.

A realistic non-conformal holographic QCD model should reveal both the spontaneous chiral symmetry breaking and color charge confinement or linear confinement, which are two main features of QCD in the low energy regime. In the top-down approach, the Sakai-Sugimoto (SS) model or $D_4 - D_8$ brane system [66, 67] is one of the most successful non-conformal holographic QCD models. In the bottom-up approach, the dynamical holographic QCD (DhQCD) model constructed in Refs. [118–120] can simultaneously describe both chiral symmetry breaking and linear confinement, where the gluon dynamics background is solved by the coupling between the graviton and the dilaton field $\Phi(z)$, which is responsible for the gluon condensate and confinement, and the scalar field $X(z)$ is introduced to mimic chiral dynamics. Evolution of the dilaton field and scalar field in 5-dimensional space-time resemble the renormalization group from ultraviolet (UV) to infrared (IR). This dynamical holographic QCD model describes the scalar glueball spectra and the light meson spectral quite well [118–120]. Further studies [121–123] show that this dynamical holographic QCD model can also describe QCD phase transition, equation of state of QCD matter and temperature dependent transport properties, including shear viscosity, bulk viscosity, electric conductivity as well as jet quenching parameter. Except the dynamical holographic QCD model, there are several other non-conformal holographic QCD models in the same graviton-dilaton system which can well describe non-perturbative QCD properties, e.g. the Gubser model [124–126] and the improved holographic QCD model [127–129] with inputting of a dilaton potential, and the refined model [130] and Dudal model [131] with inputting of a deformed metric.

In the graviton-dilaton system, the metric, the dilaton field and the dilaton potential are self-consistently solved from each other through the Einstein field equations and the equation of motion of the dilaton field. In principle, the three types of models, A) inputting the form of the dilaton field, B) inputting the deformed metric, and C) inputting the dilaton potential, should be equivalent to describe the background at zero temperature and zero density. We will compare the glueball including (scalar, vector as well as tensor glueballs and their excitations) and oddball spectra, and compare thermodynamical properties with lattice QCD results for pure gluon system and/or $2 + 1$ flavors system in these three types of models.

The paper is organized as following: we introduce the general Einstein-Maxwell-dilaton framework in section 2. Then in section 3 we introduce five different models in the graviton-dilaton system. In section 4 we introduce the glueball and oddball operator and calculate the mass spectra in these models and we compare the results of mass spectra with lattice results, results from QCD sum rule and results extracted from high energy scattering data. In section 5 we compare thermodynamical properties of these models with lattice results. Finally, a short summary is given in section 6.

2 The general Einstein-Maxwell-dilaton system

To keep the self-consistency of investigating the glueball spectra as well as further studies on QCD matter at finite temperature and finite chemical potential, we firstly introduce the general framework of the Einstein-Maxwell-dilaton (EMD) system, which comes back to the graviton-dilaton coupling system at zero chemical potential. The total action of 5-dimensional holographic QCD model including glueball/oddball excitations takes the following form:

$$S_{\text{total}}^s = S_b^s + S_g^s, \quad (2.1)$$

where S_b^s is the action for the background in the string frame, and S_g^s is the action describing glueballs in the string frame.

The Einstein-Maxwell-dilaton action S_b^s for the background in the string frame takes the form of:

$$S_b^s = \frac{1}{2\kappa_5^2} \int d^5x \sqrt{-g^s} e^{-2\Phi} \left[R^s + 4g^{sMN} \partial_M \Phi \partial_N \Phi - V^s(\Phi) - \frac{h(\Phi)}{4} e^{\frac{4\Phi}{3}} g^{sM\tilde{M}} g^{sN\tilde{N}} F_{MN} F_{\tilde{M}\tilde{N}} \right], \quad (2.2)$$

where s denotes the string frame, $\kappa_5^2 = 8\pi G_5$, the G_5 is the 5-dimensional Newton constant. The g^s is the determinant of the metric in the string frame: $g^s = \det(g_{MN})$, and the metric tensor in the string frame is extracted from

$$ds^2 = \frac{L^2 e^{2A_s(z)}}{z^2} \left(-f(z) dt^2 + \frac{dz^2}{f(z)} + dy_1^2 + dy_2^2 + dy_3^2 \right), \quad (2.3)$$

where L is the curvature radius of the asymptotic AdS_5 space-time. For simplicity, we set $L = 1$ in the following calculations. The R^s is the Ricci curvature scalar in the string frame. The scalar field $\Phi(z)$ is the dilaton field which depends only on the coordinate z , F_{MN} is the field strength of the $U(1)$ gauge field A_M :

$$F_{MN} = \partial_M A_N - \partial_N A_M. \quad (2.4)$$

The 5-dimensional field A_M is dual to baryon number current. $h(\Phi)$ describes the coupling strength of A_M in the theory, $V^s(\Phi)$ represents the potential of the dilaton field in the string frame. $h(\Phi)$ and $V^s(\Phi)$ are the functions that depends only on the value of Φ .

2.1 The Einstein-Maxwell-dilaton system in the Einstein frame

As discussed in Ref. [132], it is convenient to calculate the vacuum expectation value of the loop operator in the string frame, and it is more convenient to work out the gravity solution and to study equation of state in the Einstein frame. So we apply the Weyl transformation [133, 134]

$$g_{MN}^s = e^{\frac{4\Phi}{3}} g_{MN}^E \quad (2.5)$$

to Eq. (2.2). Here g_{MN}^E is the metric tensor in the Einstein frame, the capital letter 'E' denotes the Einstein frame. Then, Eq. (2.2) can be written as

$$S^E = \frac{1}{2\kappa_5^2} \int d^5x \sqrt{-g^E} \left[R^E - \frac{4}{3} g^{EMN} \partial_M \Phi \partial_N \Phi - V^E(\Phi) - \frac{h(\Phi)}{4} g^{EM\tilde{M}} g^{EN\tilde{N}} F_{MN} F_{\tilde{M}\tilde{N}} \right], \quad (2.6)$$

with $V^E = e^{\frac{4}{3}\Phi} V^s$.

Then we define a new dilaton field ϕ :

$$\phi = \sqrt{\frac{8}{3}} \Phi. \quad (2.7)$$

Now Eq. (2.6) becomes

$$S^E = \frac{1}{2\kappa_5^2} \int d^5x \sqrt{-g^E} \left[R^E - \frac{1}{2} g^{EMN} (\partial_M \phi) (\partial_N \phi) - V_\phi(\phi) - \frac{h_\phi(\phi)}{4} g^{EM\tilde{M}} g^{EN\tilde{N}} F_{MN} F_{\tilde{M}\tilde{N}} \right], \quad (2.8)$$

where $V_\phi(\phi) = V^E(\Phi)$, and $h_\phi(\phi) = h(\Phi)$. According to Eqs. (2.3), (2.5) and (2.7), we can derive the line element in Einstein frame:

$$ds^2 = \frac{L^2 e^{2A_E(z)}}{z^2} \left(-f(z) dt^2 + \frac{dz^2}{f(z)} + dy_1^2 + dy_3^2 + dy_3^2 \right), \quad (2.9)$$

where

$$A_E(z) = A_s(z) - \sqrt{\frac{1}{6}} \phi(z). \quad (2.10)$$

After applying variation to Eq. (2.8), we can derive the Einstein field equations and the equations of motion of A_M and ϕ as follows

$$\begin{aligned} R_{MN}^E - \frac{1}{2} g_{MN}^E R^E - T_{MN} &= 0, \\ \nabla_M [h_\phi(\phi) F^{MN}] &= 0, \\ \partial_M [\sqrt{-g} \partial^M \phi] - \sqrt{-g} \left(\frac{dV_\phi(\phi)}{d\phi} + \frac{F^2}{4} \frac{dh_\phi(\phi)}{d\phi} \right) &= 0, \end{aligned} \quad (2.11)$$

with the energy-momentum tensor T_{MN}

$$\begin{aligned} T_{MN} &= \frac{1}{2} \left[(\partial_M \phi) (\partial_N \phi) - \frac{1}{2} g_{MN}^E g^{P\tilde{P}} (\partial_P \phi) (\partial_{\tilde{P}} \phi) - g_{MN}^E V_\phi(\phi) \right] \\ &\quad + \frac{h_\phi(\phi)}{2} \left(g^{E P \tilde{P}} F_{MP} F_{N\tilde{P}} - \frac{1}{4} g_{MN}^E g^{E P \tilde{P}} g^{E Q \tilde{Q}} F_{PQ} F_{\tilde{P}\tilde{Q}} \right). \end{aligned} \quad (2.12)$$

We can safely suppose all the components of $A_M(z)$ are zero except $A_t(z)$. Substituting Eq. (2.9) into the EOMs Eq. (2.11), we then derive the EOMs for the components:

$$A_t'' + A_t' \left(-\frac{1}{z} + \frac{h_\phi'}{h_\phi} + A_E' \right) = 0, \quad (2.13)$$

$$f'' + f' \left(-\frac{3}{z} + 3A_E' \right) - \frac{e^{-2A_E} A_t'^2 z^2 h_\phi}{L^2} = 0, \quad (2.14)$$

$$A_E'' + \frac{f''}{6f} + A_E' \left(-\frac{6}{z} + \frac{3f'}{2f} \right) - \frac{1}{z} \left(-\frac{4}{z} + \frac{3f'}{2f} \right) + 3A_E'^2 + \frac{L^2 e^{2A_E} V_\phi}{3z^2 f} = 0, \quad (2.15)$$

$$A_E'' - A_E' \left(-\frac{2}{z} + A_E' \right) + \frac{\phi'^2}{6} = 0, \quad (2.16)$$

$$\phi'' + \phi' \left(-\frac{3}{z} + \frac{f'}{f} + 3A_E' \right) - \frac{L^2 e^{2A_E}}{z^2 f} \frac{dV_\phi(\phi)}{d\phi} + \frac{z^2 e^{-2A_E} A_t'^2}{2L^2 f} \frac{dh_\phi(\phi)}{d\phi} = 0. \quad (2.17)$$

In the above 5 equations, only 4 of them are independent. Thus we can choose Eq. (2.17) as a constraint, which can be used to check the solutions.

3 Five different models in the EMD system

In the dilaton-graviton system, the metric, the dilaton field and the dilaton potential can be self-consistently solved from each other through the Einstein field equations and the equation of motion of the dilaton field. At zero temperature and zero chemical potential, the function $f(z) = 1$ and $A_t(z) = 0$, then Eq. (2.13) to Eq. (2.17) can be simplified:

$$A_E'' - \frac{6}{z} A_E' + \frac{4}{z^2} + 3A_E'^2 + \frac{L^2 e^{2A_E} V_\phi}{3z^2} = 0, \quad (3.1)$$

$$A_E'' - A_E' \left(-\frac{2}{z} + A_E' \right) + \frac{\phi'^2}{6} = 0, \quad (3.2)$$

$$\phi'' + \phi' \left(-\frac{3}{z} + 3A_E' \right) - \frac{L^2 e^{2A_E}}{z^2} \frac{dV_\phi(\phi)}{d\phi} = 0, \quad (3.3)$$

where Eq. (3.3) is the constraint. Under the condition that we have proper boundary conditions, if we input A) the form of the dilaton field $\phi(z)$, or B) the function $A_E(z)$, or C) the dilaton potential $V_\phi(\phi)$, we can solve the other two. In principle, these three types of models of EMD system are totally equivalent to describe the background in the vacuum. However, at finite temperature and finite chemical potential, the situation will become different. If we input $V_\phi(\phi)$, the form of $V_\phi(\phi)$ is independent of the temperature/chemical potential, from Eq. (2.13) and Eq. (2.17), we can solve different functions $A_E(z)$ and $\phi(z)$ at different temperature/chemical potential, which can be denoted as $A_{E,T,\mu}(T, \mu, z)$ and $\phi_{T,\mu}(T, \mu, z)$. On the other hand, if we input $A_E(z)$ (or $\phi(z)$), whose form is independent of temperature/chemical potential, we can derive $V_\phi(\phi)$ with temperature/chemical potential dependence, which can be denoted as $V_{\phi,T,\mu}(T, \mu, \phi)$. The two descriptions, that are equivalent at vacuum, now become distinct from each other at finite temperature/chemical potential. From now on, we call fixing $V_\phi(\phi)$ "description A", fixing $A_E(z)$ or $\phi(z)$ is denoted by "description B".

It is more convenient to solve the system in the Einstein frame from Eqs. (3.1) ~ (3.3). In the following we list two sets of vacuum solutions of $V_\phi(\phi)$, $A_E(z)$ and $\phi(z)$ that satisfy the EOMs.

3.1 Vacuum solutions: set I

From the experiences in Refs. [130, 131], we can input the function $A_E(z)$ in the Einstein frame, and solve $V_\phi(\phi)$ and $\phi(z)$. The simplest ansatz for the deformed metric is $A_E(z) = -az^2$, and from Eqs. (3.1) ~ (3.3) one can derive the solution as following:

$$A_E(z) = -az^2, \quad (3.4)$$

$$V_\phi(\phi) = -\frac{6}{L^2} e^{2(k(\phi))^2} \left(6 (k(\phi))^4 + 5 (k(\phi))^2 + 2 \right), \quad (3.5)$$

$$\phi(z) = z \sqrt{3a(3 + 2az^2)} + \frac{3}{2} \sqrt{6} \operatorname{arcsinh} \left[\sqrt{\frac{2a}{3}} z \right], \quad (3.6)$$

where the auxiliary function $k(\varphi)$ is defined as the inverse function of

$$\varphi(\mathfrak{z}) = \mathfrak{z} \sqrt{3(3 + 2\mathfrak{z}^2)} + \frac{3}{2} \sqrt{6} \operatorname{arcsinh} \left[\sqrt{\frac{2}{3}} \mathfrak{z} \right], \quad (3.7)$$

which means $k(\varphi(\mathfrak{z})) = \mathfrak{z}$ with $\mathfrak{z} = \sqrt{a}z$. Starting from any of the above three functions, together with proper boundary conditions, we can solve other two functions from Eq. (3.1) and Eq. (3.2).

From Eq. (3.6) we know that $\phi(z=0) = 0$, $\lim_{z \rightarrow +\infty} \phi(z) \rightarrow +\infty$. At UV boundary ($z \rightarrow 0$), the asymptotic forms of $V_\phi(\phi)$ and ϕ are given below:

$$\begin{aligned} L^2 V_\phi(\phi \rightarrow 0) = & -12 - \frac{3}{2} \phi^2 - \frac{1}{12} \phi^4 - \frac{377}{174960} \phi^6 - \frac{977}{33067440} \phi^8 - \frac{53483}{214277011200} \phi^{10} \\ & - \frac{1564351}{1145524901875200} \phi^{12} + \mathcal{O}(\phi^{14}), \end{aligned} \quad (3.8)$$

$$\begin{aligned} \phi(z \rightarrow 0) = & 6\sqrt{a}z + \frac{2}{3} a^{\frac{3}{2}} z^3 - \frac{1}{15} a^{\frac{5}{2}} z^5 + \frac{1}{63} a^{\frac{7}{2}} z^7 - \frac{5}{972} a^{\frac{9}{2}} z^9 + \frac{7}{3564} a^{\frac{11}{2}} z^{11} \\ & - \frac{7}{8424} a^{\frac{13}{2}} z^{13} + \mathcal{O}(z^{15}). \end{aligned} \quad (3.9)$$

From the UV asymptotic form of $V_\phi(\phi)$, we can extract the 5-dimensional mass square of ϕ

$$M_\phi^2 = -3. \quad (3.10)$$

According to the mass-dimension relationship $M^2 = (\Delta - p)(\Delta + p - 4)$ and $p = 0$, the dimension

$$\Delta_{\phi_-} = 1, \quad \Delta_{\phi_+} = 3. \quad (3.11)$$

At IR boundary ($z \rightarrow +\infty$), $V_\phi(\phi)$ and $\phi(z)$ behave as

$$L^2 V_\phi(\phi \rightarrow +\infty) = -\frac{27}{4} \left(\frac{3}{8} \right)^{\frac{1}{4}} e^{-\frac{3}{2} e^{\frac{\sqrt{6}}{3} \phi} + \dots} \left(\phi^{\frac{1}{2}} + \dots \right), \quad (3.12)$$

$$\begin{aligned} \phi(z \rightarrow +\infty) = \sqrt{6} & \left[az^2 + \frac{3}{4} \left(1 + \ln \left(\frac{8}{3} \right) + \ln (az^2) \right) + \frac{9}{32} \frac{1}{az^2} - \frac{27}{256} \frac{1}{a^2 z^4} + \frac{135}{2048} \frac{1}{a^3 z^6} \right. \\ & \left. - \frac{1701}{32768} \frac{1}{a^4 z^8} + \frac{15309}{327680} \frac{1}{a^5 z^{10}} - \frac{24057}{524288} \frac{1}{a^6 z^{12}} + \mathcal{O} \left(\frac{1}{z^{14}} \right) \right]. \end{aligned} \quad (3.13)$$

Eq. (3.5) lead to the masses of glueballs m_n behave as

$$m_n \sim n^{\frac{1}{2}}, \quad \text{when } n \rightarrow +\infty. \quad (3.14)$$

which shows the linear Regge behavior along n .

3.2 Vacuum solutions: set II

As for another set of solution, we start from the form of $\phi(z)$. One simple but nontrivial ansatz is to take the quadratic form of $\phi(z)$: $\phi(z) = bz^2$. As discussed in Refs. [118–120, 132], the quadratic form of the dilaton field is dual to a dimension-2 gluon condensation operator, which is responsible for the linear confinement of the gluon system. Then the solution $V_\phi(\phi)$, $A_E(z)$ and $\phi(z)$ take the form of

$$\phi(z) = bz^2, \quad (3.15)$$

$$V_\phi(\phi) = \frac{1}{L^2} 2 \times 2^{\frac{3}{4}} \times 3^{\frac{1}{4}} \phi^{\frac{3}{2}} \left[\Gamma \left(\frac{5}{4} \right) \right]^2 \left\{ \left[I_{\frac{1}{4}} \left(\frac{\phi}{\sqrt{6}} \right) \right]^2 - 4 \left[I_{-\frac{3}{4}} \left(\frac{\phi}{\sqrt{6}} \right) \right]^2 \right\}, \quad (3.16)$$

$$A_E(z) = -\ln \left[\frac{2^{\frac{3}{8}} \times 3^{\frac{1}{8}} \Gamma \left(\frac{5}{4} \right) I_{\frac{1}{4}} \left(\frac{bz^2}{\sqrt{6}} \right)}{b^{\frac{1}{4}} \sqrt{z}} \right], \quad (3.17)$$

where $\Gamma(z)$ is the Euler gamma function, $I_n(z)$ is the modified Bessel function of the first kind.

From Eq. (3.15) we know that $\phi(z=0) = 0$, $\lim_{z \rightarrow +\infty} \phi(z) \rightarrow +\infty$. At UV boundary ($z \rightarrow 0$), the asymptotic form are

$$\begin{aligned} L^2 V_\phi(\phi \rightarrow 0) = & -12 - 2\phi^2 - \frac{4}{15}\phi^4 - \frac{49}{6075}\phi^6 - \frac{11}{94770}\phi^8 - \frac{11}{11153700}\phi^{10} \\ & - \frac{38}{6851160225}\phi^{12} + \mathcal{O}(\phi^{14}), \end{aligned} \quad (3.18)$$

$$A_E(z \rightarrow 0) = -\frac{1}{30}b^2 z^4 + \frac{1}{4050}b^4 z^8 - \frac{4}{1184625}b^6 z^{12} + \mathcal{O}(z^{16}). \quad (3.19)$$

From the UV asymptotic form of $V_\phi(\phi)$, we can extract the 5-dimensional mass square of ϕ

$$M_\phi^2 = -4. \quad (3.20)$$

According to the mass-dimension relationship $M^2 = (\Delta - p)(\Delta + p - 4)$ and $p = 0$, the dimension

$$\Delta_{\phi-} = \Delta_{\phi+} = 2. \quad (3.21)$$

At IR boundary ($z \rightarrow +\infty$), $V_\phi(\phi)$ and $A_E(z)$ behave as

$$\begin{aligned}
L^2 V_\phi(\phi \rightarrow \infty) = & -\frac{1}{\pi} 2^{\frac{5}{4}} \times 3^{\frac{7}{4}} \left[\Gamma\left(\frac{5}{4}\right) \right]^2 e^{\frac{\sqrt{6}}{3}\phi} \phi^{\frac{1}{2}} \left[1 - \frac{23\sqrt{6}}{48} \frac{1}{\phi} - \frac{277}{256} \frac{1}{\phi^2} - \frac{4365\sqrt{6}}{4096} \frac{1}{\phi^3} \right. \\
& - \frac{1271565}{131072} \frac{1}{\phi^4} - \frac{41182155\sqrt{6}}{2097152} \frac{1}{\phi^5} - \frac{9973379745}{33554432} \frac{1}{\phi^6} - \frac{481731815565\sqrt{6}}{536870912} \frac{1}{\phi^7} \\
& - \frac{650211981544125}{34359738368} \frac{1}{\phi^8} - \frac{41734532955290175\sqrt{6}}{549755813888} \frac{1}{\phi^9} \\
& - \frac{18065483595471987675}{8796093022208} \frac{1}{\phi^{10}} - \frac{1447278481564158318075\sqrt{6}}{140737488355328} \frac{1}{\phi^{11}} \\
& - \frac{1529878341359963470300425}{4503599627370496} \frac{1}{\phi^{12}} - \frac{146978223450520872139104375\sqrt{6}}{72057594037927936} \frac{1}{\phi^{13}} \\
& \left. + \mathcal{O}\left(\frac{1}{\phi^{14}}\right) \right] \left\{ 1 + \frac{5\sqrt{2}}{6} e^{-\frac{\sqrt{6}}{3}\phi} \left[1 + \mathcal{O}\left(\frac{1}{\phi}\right) \right] \right\}, \tag{3.22}
\end{aligned}$$

$$\begin{aligned}
A_E(z \rightarrow \infty) = & -\frac{\sqrt{6}}{6} b z^2 + \frac{3}{2} \ln(\sqrt{b} z) + \ln \left[\frac{\pi^{\frac{1}{2}}}{2^{\frac{1}{8}} 3^{\frac{3}{8}} \Gamma\left(\frac{5}{4}\right)} \right] - \frac{3\sqrt{6}}{32} \frac{1}{b z^2} - \frac{9}{32} \frac{1}{b^2 z^4} \\
& - \frac{297\sqrt{6}}{1024} \frac{1}{b^3 z^6} - \frac{1377}{512} \frac{1}{b^4 z^8} - \frac{451251\sqrt{6}}{81920} \frac{1}{b^5 z^{10}} - \frac{172287}{2048} \frac{1}{b^6 z^{12}} + \mathcal{O}\left(\frac{1}{z^{14}}\right) \\
& + \mathcal{O}\left(e^{-\frac{\sqrt{6}}{3} b z^2}\right) + \mathcal{O}\left(\frac{1}{z^2} e^{-\frac{\sqrt{6}}{3} b z^2}\right). \tag{3.23}
\end{aligned}$$

Again, from the asymptotic expansion of $V_\phi(\phi)$ at IR boundary, we can conclude that linear Regge behavior of the masses of glueballs m_n :

$$m_n^2 \sim n, \quad \text{when } n \rightarrow +\infty, \tag{3.24}$$

which shows the linear Regge behavior along n .

3.3 Five different models

The two sets of vacuum solutions listed above have linear confinement and can produce glueball bound state. Not all models can show such feature. According to Refs. [129, 135], if we require that the theory is confined and bad singularities are absent, the asymptotic behavior of $V_\phi(\phi)$ at IR boundary should be

$$\begin{aligned}
L^2 V_\phi(\phi \rightarrow +\infty) = & c_V e^{c_{\phi,1}\phi + \dots} (\phi^{c_{\phi,2}} + \dots), \\
& \begin{cases} \frac{\sqrt{6}}{3} < c_{\phi,1} < \frac{2\sqrt{3}}{3}, & c_{\phi,2} \text{ is real number,} \\ c_{\phi,1} = \frac{\sqrt{6}}{3}, & c_{\phi,2} \geq 0, \end{cases} \tag{3.25}
\end{aligned}$$

where c_V is constant. When $c_{\phi,1} = \frac{\sqrt{6}}{3}$ and $c_{\phi,2} > 0$, there are asymptotically linear glueball spectra:

$$m_n \sim n^{c_{\phi,2}} \quad \text{when } n \rightarrow +\infty. \tag{3.26}$$

For comparison, we plot three different dilaton potentials $V_\phi(\phi)$ in Fig. 1. One of them is the Gubser model taken from Ref. [126]:

$$V_\phi(\phi) = \frac{-12 \cosh(0.606\phi) + 2.057\phi^2}{L^2}, \quad (3.27)$$

the others two are Eq. (3.5) and Eq. (3.16). Here we set $L = 1$. The dashed black line is $e^{\frac{\sqrt{6}}{3}\phi}$. According to the conclusion in subsection 3.1, if the potential is more gradual than this line, such as the blue line that represents the Gubser model in Eq. (3.27), the theory is gapless and non-confining.

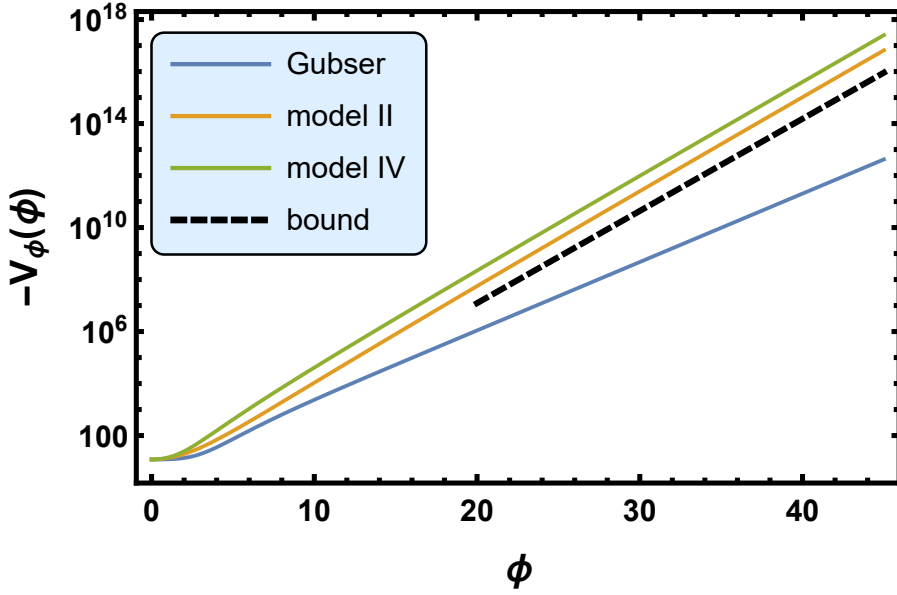


Figure 1. These are three different dilaton potentials $V_\phi(\phi)$. The longitudinal axis is the value of $-V_\phi(\phi)$ in logarithm coordinate. The horizontal axis is the value of ϕ . The dashed black line is $e^{\frac{\sqrt{6}}{3}\phi}$. The blue line, orange line and green line represent the potential in Eq. (3.27), Eq. (3.5) and Eq. (3.16) respectively. The meaning of "model II" and "model IV" will be explained later. The dashed black line is $e^{\frac{\sqrt{6}}{3}\phi}$. The bound is given by Eq.(3.26) from Refs. [129, 135]. If the potential is more gradual than this bound, the theory is gapless and non-confining.

As we stated below Eqs. (3.1) \sim (3.3), there are two different descriptions of the input of EMD system. Combining with the two different sets of vacuum solutions Eqs. (3.5) \sim (3.6) and Eq. (3.16) \sim (3.15), we consider five models in this article.

3.3.1 Model I and II

In model I, we use description-B and input $A_E(z)$ as Eq. (3.4):

$$A_E(z) = -az^2. \quad (3.28)$$

Note that the dimension of the parameter a is $[E]^2$ and its value decides the energy scale of the EMD system. At vacuum, the boundary condition is chosen as

$$\phi(z=0) = 0. \quad (3.29)$$

Combining the boundary condition Eq. (3.29) with the EOMs Eq. (3.2) and Eq. (3.1), we can solve $\phi(z)$ and $V_\phi(\phi)$. The results are Eq. (3.6) and Eq. (3.5).

As for finite temperature and finite chemical potential, the EOMs are Eq. (2.13) \sim (2.16). There may exist the black hole¹ in space-time manifold, the metric of which in conformal coordinate z is Eq. (2.9). The boundary conditions are given as

$$\begin{aligned} A_t(z=0) &= \mu, \\ A_t(z=z_h) &= 0, \\ f(z=0) &= 1, \\ f(z=z_h) &= 0, \\ \phi(z=0) &= 0, \end{aligned} \quad (3.30)$$

where $z = z_h$ is the location of the event horizon of black hole on the coordinate z , μ is the chemical potential. Besides the boundary condition Eq. (3.30), the form of $h_\phi(\phi)$ are also needed to solve the EOMs. However, we consider the $\mu = 0$ case, which means $A_t(z) = 0$ through the article. Thus our calculations and results are independent on $h_\phi(\phi)$.

In model II, we use description-A and input $V_\phi(\phi)$ as Eq. (3.5):

$$V_\phi(\phi) = -\frac{6}{L^2} e^{2(k(\phi))^2} \left(6(k(\phi))^4 + 5(k(\phi))^2 + 2 \right). \quad (3.31)$$

At vacuum, the boundary conditions are chosen as

$$A_E(z=0) = 0, \quad (3.32)$$

$$\phi(z=0) = 0, \quad (3.33)$$

$$\left. \frac{d\phi(z)}{dz} \right|_{z=0} = 6\sqrt{a}. \quad (3.34)$$

Eq. (3.32) guarantees the space-time is asymptotic AdS_5 at UV boundary. Eq. (3.34) contains a parameter a , the dimension of which is $[E]^2$ and the value of which decides the energy scale of the EMD system. Given by these boundary conditions and set the value of a in Eq. (3.34) to be the same with that in Eq. (3.28), we can solve the EOMs at vacuum, then it will be found that the solutions are totally equivalent to those in model I at vacuum.

¹Actually, the black hole may not exist for all values of temperature and chemical potential. Under some situations, it only exists above a certain temperature T_{\min} . The AdS thermal gas is the only solution below T_{\min} . However, under other situations, we always have the black hole solution.

As for finite temperature and finite chemical potential, the EOMs are Eq. (2.13) ~ (2.16). The boundary conditions are given as

$$\begin{aligned}
A_t(z=0) &= \mu, \\
A_t(z=z_h) &= 0, \\
f(z=0) &= 1, \\
f(z=z_h) &= 0, \\
A_E(z=0) &= 0, \\
\phi(z=0) &= 0, \\
\left. \frac{d\phi(z)}{dz} \right|_{z=0} &= 6\sqrt{a},
\end{aligned} \tag{3.35}$$

where $z = z_h$ is the location of the event horizon of black hole on the coordinate z , μ is the chemical potential. We should emphasize here that at finite temperature or finite chemical potential case, the solutions here are different from those in model I.

3.3.2 Model III and IV

In model III, we use description B and input $\phi(z)$ as Eq. (3.15):

$$\phi(z) = bz^2. \tag{3.36}$$

Note that the dimension of the parameter b is $[E]^2$ and its value decides the energy scale of the EMD system. Substituting Eq. (3.36) into Eq. (3.2), we can solve a general solution for $A_E(z)$ with two integration constants. However, the value of this general solution is usually complex. If we force the reality of $A_E(z)$ and consider the boundary condition

$$A_E(z=0) = 0, \tag{3.37}$$

we can solve $A_E(z)$ and $V_\phi(\phi)$. The results are Eq. (3.17) and Eq. (3.15).

As for finite temperature and finite chemical potential, the EOMs are Eqs. (2.13) ~ (2.16). The boundary conditions are imposed as

$$\begin{aligned}
A_t(z=0) &= \mu, \\
A_t(z=z_h) &= 0, \\
f(z=0) &= 1, \\
f(z=z_h) &= 0,
\end{aligned} \tag{3.38}$$

where $z = z_h$ is the location of the event horizon of black hole on the coordinate z , μ is the chemical potential. Collecting these boundary conditions and Eq. (3.36), Eq. (3.17), we can then solve the EMD system.

In model IV, we use description A and input $V_\phi(\phi)$ as Eq. (3.16):

$$V_\phi(\phi) = \frac{1}{L^2} 2 \times 2^{\frac{3}{4}} \times 3^{\frac{1}{4}} \phi^{\frac{3}{2}} \left[\Gamma\left(\frac{5}{4}\right) \right]^2 \left\{ \left[I_{\frac{1}{4}}\left(\frac{\phi}{\sqrt{6}}\right) \right]^2 - 4 \left[I_{-\frac{3}{4}}\left(\frac{\phi}{\sqrt{6}}\right) \right]^2 \right\}. \tag{3.39}$$

At vacuum, the boundary conditions are chosen as

$$A_E(z=0) = 0, \quad (3.40)$$

$$\lim_{z \rightarrow 0} \frac{\phi(z)}{z^2} = b, \quad (3.41)$$

Again, we force that $A_E(z)$ is real. The Eq. (3.40) guarantees the space-time is asymptotic AdS_5 at UV boundary. Eq. (3.41) contains a parameter b , the dimension of which is $[E]^2$ and the value of which decides the energy scale of the EMD system. Given by these boundary conditions and set the value of b in Eq. (3.41) to be the same with that in Eq. (3.36), we can solve the EOMs at vacuum, then it will be found that the solutions are totally equivalent to those in model III at vacuum.

As for finite temperature and finite chemical potential, the EOMs are Eqs. (2.13) \sim (2.16). The boundary conditions are given as

$$\begin{aligned} A_t(z=0) &= \mu, \\ A_t(z=z_h) &= 0, \\ f(z=0) &= 1, \\ f(z=z_h) &= 0, \\ A_E(z=0) &= 0, \\ \phi(z=0) &= 0. \end{aligned} \quad (3.42)$$

Given by these boundary conditions, we still have the freedom to choose the energy scale of the EMD system. We should emphasis here that at finite temperature or finite chemical potential case, the solutions here are different from those in model III.

3.3.3 Model V

In model V, we input $\phi(z)$ as

$$\phi(z) = \frac{2\sqrt{6}}{3} z \sqrt{3d(3+2dz^2)} + 6 \operatorname{arcsinh} \left[\sqrt{\frac{2d}{3}} z \right]. \quad (3.43)$$

Note that the dimension of the parameter d is $[E]^2$ and its value decides the energy scale of the EMD system. Substituting Eq. (3.43) into Eq. (3.2), we force the reality of $A_E(z)$ and consider the boundary condition

$$A_E(z=0) = 0, \quad (3.44)$$

we can solve $A_E(z)$ and $V_\phi(\phi)$ numerically. Although we can't get the analytical form of $A_E(z)$, we can still can derive its asymptotic expansions:

$$\begin{aligned} A_E(z \rightarrow 0) &= -\frac{8}{3} dz^2 + \frac{8}{9} d^2 z^4 - \frac{512}{567} d^3 z^6 + \frac{1664}{1701} d^4 z^8 - \frac{311296}{280665} d^5 z^{10} \\ &\quad + \frac{19972096}{15324309} d^6 z^{12} + \mathcal{O}(z^{14}), \end{aligned} \quad (3.45)$$

As for finite temperature and finite chemical potential, the EOMs are Eqs. (2.13) ~ (2.16). The boundary conditions are imposed as

$$\begin{aligned} A_t(z=0) &= \mu, \\ A_t(z=z_h) &= 0, \\ f(z=0) &= 1, \\ f(z=z_h) &= 0, \end{aligned} \tag{3.46}$$

where $z = z_h$ is the location of the event horizon of black hole on the coordinate z , μ is the chemical potential. Collecting these boundary conditions, the Eq. (3.43), and the numerical solution of $A_E(z)$, we can then solve the EMD system.

4 Spectra of glueballs and oddballs

In this section, we discuss the spectra of glueballs and oddballs. In our treatment, the 5-dimensional fields dual to glueballs/oddballs are excited from the background. The action describing scalar, vector, and tensor glueballs/oddballs in the string frame is

$$\begin{aligned} S_g^s = -c_g \int d^5x \sqrt{-g_s} e^{-p\Phi} \Bigg\{ & \left[\frac{1}{2} g^{sMN} \partial_M \mathcal{S}(z) \partial_N \mathcal{S} + \frac{1}{2} e^{-c_{r.m.}\Phi} M_{\mathcal{S},5}^2 \mathcal{S}^2 \right] \\ & + \left[\frac{1}{4} g^{sM\tilde{M}} g^{sN\tilde{N}} (\partial_M \mathcal{V}_N - \partial_N \mathcal{V}_M) (\partial_{\tilde{M}} \mathcal{V}_{\tilde{N}} - \partial_{\tilde{N}} \mathcal{V}_{\tilde{M}}) \right. \\ & \quad \left. + \frac{1}{2} e^{-c_{r.m.}\Phi} M_{\mathcal{V},5}^2 \mathcal{V}^2 \right] \\ & + \left[\frac{1}{2} \nabla_L \mathcal{T}_{MN} \nabla^L \mathcal{T}^{MN} - \nabla_L \mathcal{T}^{LM} \nabla^N \mathcal{T}_{NM} \right. \\ & \quad + \nabla_M \mathcal{T}^{MN} \nabla_N \mathcal{T} - \frac{1}{2} \nabla_M \mathcal{T} \nabla^M \mathcal{T} \\ & \quad \left. + \frac{1}{2} e^{-c_{r.m.}\Phi} M_{\mathcal{T},5}^2 (\mathcal{T}^{MN} h_{MN} - \mathcal{T}^2) \right] \\ & \left. + \text{terms for high spin fields (spin } S \geq 3) \right\}, \end{aligned} \tag{4.1}$$

where s denotes the string frame, c_g describes the coupling strength of glueballs part in the whole theory. The fields \mathcal{S} , \mathcal{V}_M , and \mathcal{T}_{MN} are 5-dimensional fields that are dual to scalar glueball, vector glueball, and spin-2 glueball operators respectively. $\mathcal{T} = g^{sMN} \mathcal{T}_{MN}$, and \mathcal{T}_{MN} satisfies the following constraints

$$\nabla_M \mathcal{T}^{MN} = 0, \quad \mathcal{T} = 0, \quad \mathcal{T}_{\mu\nu} = \frac{1}{z^2} e^{2A_s} \mathcal{T}_{\mu\nu}, \quad \mathcal{T}_{Mz} = 0. \tag{4.2}$$

As in Ref. [136], the parameter p is introduced to make a distinction between glueballs (oddballs) with different P-parity:

$$\begin{cases} p = 1, & \text{for even parity,} \\ p = -1, & \text{for odd parity.} \end{cases} \tag{4.3}$$

Also we introduce a z dependent modified 5-dimensional mass:

$$M_5^2(z) = e^{-c_{r.m.}\Phi} M_5^2, \quad (4.4)$$

where $c_{r.m.}$ is a constant. The M_5^2 is listed in Table 1 given by the $\text{AdS}_5/\text{CFT}_4$ correspondence dictionary. The $\text{AdS}_5/\text{CFT}_4$ duality gives one-to-one correspondence between 4-dimensional operators in the $\mathcal{N} = 4$ Super Yang-Mills theory and the spectrum of the type IIB string theory on $\text{AdS}_5 \times S^5$. Based on the AdS/CFT dictionary, the conformal dimension of a p -form operator at the ultraviolet (UV) boundary is related to the 5-dimensional mass square M_5^2 of its dual field in the bulk as follows [56–58] :

$$M_5^2 = (\Delta - p)(\Delta + p - 4). \quad (4.5)$$

4.1 Glueballs and oddballs

In the bottom-up holographic QCD models, one can expect a more general correspondence, i.e. each 4-dimensional operator $\mathcal{O}(x)$ corresponds to a 5-dimensional field $O(x, z)$ in the bulk theory. To investigate the glueball spectra, we consider the lowest dimension operators with the corresponding quantum numbers defined in the field theory living on the 4-dimensional boundary. We show the C-even/odd glueball and oddball operators and their corresponding 5-dimensional mass square in Table 1.

J^{PC}	4-dimensional operator: $\mathcal{O}(x)$	Δ	p	M_5^2
0^{++}	$\text{Tr}(G^2) = \vec{E}^a \cdot \vec{E}^a - \vec{B}^a \cdot \vec{B}^a$	4	0	0
0^{-+}	$\text{Tr}(G\vec{G}) = \vec{E}^a \cdot \vec{B}^a$	4	0	0
0^{+-}	$\text{Tr}(\{(D_\tau G_{\mu\nu}), (D_\tau G_{\rho\nu})\} (D_\mu G_{\rho\alpha}))$	9	0	45
0^{--}	$\text{Tr}(\{(D_\tau G_{\mu\nu}), (D_\tau G_{\rho\nu})\} (D_\mu \tilde{G}_{\rho\alpha}))$	9	0	45
1^{-+}	$f^{abc} \partial_\mu [G_{\mu\nu}^a] [G_{\nu\rho}^b] [G_{\rho\alpha}^c], f^{abc} \partial_\mu [G_{\mu\nu}^a] [\tilde{G}_{\nu\rho}^b] [\tilde{G}_{\rho\alpha}^c],$ $f^{abc} \partial_\mu [\tilde{G}_{\mu\nu}^a] [G_{\nu\rho}^b] [\tilde{G}_{\rho\alpha}^c], f^{abc} \partial_\mu [\tilde{G}_{\mu\nu}^a] [\tilde{G}_{\nu\rho}^b] [G_{\rho\alpha}^c]$	7	1	24
1^{+-}	$d^{abc} (\vec{E}_a \cdot \vec{E}_b) \vec{B}_c$	6	1	15
1^{--}	$d^{abc} (\vec{E}_a \cdot \vec{E}_b) \vec{E}_c$	6	1	15
2^{++}	$E_i^a E_j^a - B_i^a B_j^a - \text{trace}$	4	2	4
2^{-+}	$E_i^a B_j^a + B_i^a E_j^a - \text{trace}$	4	2	4
2^{+-}	$d^{abc} \mathcal{S} \left[E_a^i (\vec{E}_b \times \vec{B}_c)^j \right]$	6	2	16
2^{--}	$d^{abc} \mathcal{S} \left[B_a^i (\vec{E}_b \times \vec{B}_c)^j \right]$	6	2	16
3^{+-}	$d^{abc} \mathcal{S} \left[B_a^i B_b^j B_c^k \right]$	6	3	15
3^{--}	$d^{abc} \mathcal{S} \left[E_a^i E_b^j E_c^k \right]$	6	3	15

Table 1. 5-dimensional mass square of C-even glueballs and C-odd oddballs. The operators are taken from Refs. [27, 31, 32, 85].

The lowest dimension gauge invariant three-gluon currents that couple to the exotic 0^{+-} and 0^{--} glueballs are constructed in Ref. [31]:

$$j_\alpha^{0^{+-}}(x) = g_s^3 \text{Tr} \left(\{ (D_\tau G_{\mu\nu}(x)), (D_\tau G_{\rho\nu}(x)) \} (D_\mu G_{\rho\alpha}(x)) \right), \quad (4.6)$$

$$j_\alpha^{0^{--}}(x) = g_s^3 \text{Tr} \left(\{ (D_\tau G_{\mu\nu}(x)), (D_\tau G_{\rho\nu}(x)) \} (D_\mu \tilde{G}_{\rho\alpha}(x)) \right). \quad (4.7)$$

For trigluon glueball 1^{-+} , and 2^{+-} , the currents that match the unconventional quantum number and satisfy the constraints of the gauge invariance are given in Refs. [27]:

$$\begin{aligned} j_\alpha^{1^{-+},A}(x) &= g_s^3 f^{abc} \partial_\mu [G_{\mu\nu}^a(x)] [G_{\nu\rho}^b(x)] [G_{\rho\alpha}^c(x)], \\ j_\alpha^{1^{-+},B}(x) &= g_s^3 f^{abc} \partial_\mu [G_{\mu\nu}^a(x)] [\tilde{G}_{\nu\rho}^b(x)] [\tilde{G}_{\rho\alpha}^c(x)], \\ j_\alpha^{1^{-+},C}(x) &= g_s^3 f^{abc} \partial_\mu [\tilde{G}_{\mu\nu}^a(x)] [G_{\nu\rho}^b(x)] [\tilde{G}_{\rho\alpha}^c(x)], \\ j_\alpha^{1^{-+},D}(x) &= g_s^3 f^{abc} \partial_\mu [\tilde{G}_{\mu\nu}^a(x)] [\tilde{G}_{\nu\rho}^b(x)] [G_{\rho\alpha}^c(x)], \end{aligned} \quad (4.8)$$

and

$$\begin{aligned} j_{\mu\alpha}^{2^{+-},A}(x) &= g_s^3 d^{abc} [G_{\mu\nu}^a(x)] [G_{\nu\rho}^b(x)] [G_{\rho\alpha}^c(x)], \\ j_{\mu\alpha}^{2^{+-},B}(x) &= g_s^3 d^{abc} [G_{\mu\nu}^a(x)] [\tilde{G}_{\nu\rho}^b(x)] [\tilde{G}_{\rho\alpha}^c(x)], \\ j_{\mu\alpha}^{2^{+-},C}(x) &= g_s^3 d^{abc} [\tilde{G}_{\mu\nu}^a(x)] [G_{\nu\rho}^b(x)] [\tilde{G}_{\rho\alpha}^c(x)], \\ j_{\mu\alpha}^{2^{+-},D}(x) &= g_s^3 d^{abc} [\tilde{G}_{\mu\nu}^a(x)] [\tilde{G}_{\nu\rho}^b(x)] [G_{\rho\alpha}^c(x)], \end{aligned} \quad (4.9)$$

where d^{abc} stands for the totally symmetric $SU_c(3)$ structure constant and $g_{\alpha\beta}^t = g_{\alpha\beta} - \partial_\alpha \partial_\beta / \partial^2$.

4.2 Equation of motion for scalar, vector and tensor glueballs/oddballs

From the 5-dimensional action for the glueball/oddball in the string frame Eq. (4.1), we can derive the equation of motion for the glueballs. The equation of motion for the scalar glueballs \mathcal{S} is given as:

$$\begin{aligned} & -z^3 e^{-(3A_s - p\Phi)} \partial_z \left[\frac{1}{z^3} e^{3A_s - p\Phi} \partial_z \mathcal{S}_n \right] \\ & + \frac{1}{z^2} e^{2A_s} e^{-c_{r.m.}\Phi} M_{\mathcal{S},5}^2 \mathcal{S}_n = m_{\mathcal{S},n}^2 \mathcal{S}_n. \end{aligned} \quad (4.10)$$

Via the substitution

$$\mathcal{S}_n \rightarrow z^{\frac{3}{2}} e^{-\frac{1}{2}(3A_s - p\Phi)} \mathcal{S}_n, \quad (4.11)$$

the equation can be brought into Schrödinger-like equation

$$-\mathcal{S}_n'' + V_{\mathcal{S}} \mathcal{S}_n = m_{\mathcal{S},n}^2 \mathcal{S}_n, \quad (4.12)$$

with the 5-dimensional effective Schrödinger potential

$$V_{\mathcal{V}} = \frac{3A_s'' + \frac{3}{z^2} - p\Phi''}{2} + \frac{\left[3A_s' - \frac{3}{z} - p\Phi'\right]^2}{4} + \frac{1}{z^2}e^{2A_s}e^{-c_{r.m.}\Phi}M_{\mathcal{V},5}^2. \quad (4.13)$$

The equation of motion for the vector glueballs \mathcal{V}_M is given as:

$$-ze^{-(A_s-p\Phi)}\partial_z\left[\frac{1}{z}e^{A_s-p\Phi}\partial_z\mathcal{V}_n\right] + \frac{1}{z^2}e^{2A_s}e^{-c_{r.m.}\Phi}M_{\mathcal{V},5}^2\mathcal{V}_n = m_{\mathcal{V},n}^2\mathcal{V}_n. \quad (4.14)$$

Via the substitution

$$\mathcal{V}_n \rightarrow z^{\frac{1}{2}}e^{-\frac{1}{2}(A_s-p\Phi)}\mathcal{V}_n, \quad (4.15)$$

the equation can be brought into Schrödinger-like equation

$$-\mathcal{V}_n'' + V_{\mathcal{V}}\mathcal{V}_n = m_{\mathcal{V},n}^2\mathcal{V}_n, \quad (4.16)$$

with the 5-dimensional effective Schrödinger potential

$$V_{\mathcal{V}} = \frac{A_s'' + \frac{1}{z^2} - p\Phi''}{2} + \frac{\left[A_s' - \frac{1}{z} - p\Phi'\right]^2}{4} + \frac{1}{z^2}e^{2A_s}e^{-c_{r.m.}\Phi}M_{\mathcal{V},5}^2. \quad (4.17)$$

The equation of motion for the spin-2 glueballs \mathcal{T}_{MN} is given as

$$-z^3e^{-(3A_s-p\Phi)}\partial_z\left[\frac{1}{z^3}e^{3A_s-p\Phi}\partial_z\mathcal{T}_n\right] + \frac{1}{z^2}e^{2A_s}e^{-c_{r.m.}\Phi}M_{\mathcal{T},5}^2\mathcal{T}_n = m_{\mathcal{T},n}^2\mathcal{T}_n. \quad (4.18)$$

Via the substitution

$$\mathcal{T}_n \rightarrow z^{\frac{3}{2}}e^{-\frac{1}{2}(3A_s-p\Phi)}\mathcal{T}_n, \quad (4.19)$$

the equation can be brought into Schrödinger-like equation

$$-\mathcal{T}_n'' + V_{\mathcal{T}}\mathcal{T}_n = m_{\mathcal{T},n}^2\mathcal{T}_n, \quad (4.20)$$

with the 5-dimensional effective Schrödinger potential

$$V_{\mathcal{T}} = \frac{3A_s'' + \frac{3}{z^2} - p\Phi''}{2} + \frac{\left[3A_s' - \frac{3}{z} - p\Phi'\right]^2}{4} + \frac{1}{z^2}e^{2A_s}e^{-c_{r.m.}\Phi}M_{\mathcal{T},5}^2. \quad (4.21)$$

According to Ref. [65], the equation of motion for the high spin glueballs $\mathcal{H}_{M_1M_2\dots M_S}$, the spin S of which are larger than 2, is given as

$$\begin{aligned} & -z^{2S-1}e^{-[(2S-1)A_s-p\Phi]}\partial_z\left[\frac{1}{z^{2S-1}}e^{(2S-1)A_s-p\Phi}\partial_z\mathcal{H}_n\right] \\ & + \frac{1}{z^2}e^{2A_s}e^{-c_{r.m.}\Phi}M_{\mathcal{H},5}^2\mathcal{H}_n = m_{\mathcal{H},n}^2\mathcal{H}_n, \end{aligned} \quad (4.22)$$

where $S \geq 3$. Via the substitution

$$\mathcal{H}_n \rightarrow z^{\frac{2S-1}{2}}e^{-\frac{1}{2}[(2S-1)A_s-p\Phi]}\mathcal{H}_n, \quad (4.23)$$

the equation can be brought into Schrödinger-like equation

$$-\mathcal{H}_n'' + V_{\mathcal{H}} \mathcal{H}_n = m_{\mathcal{H},n}^2 \mathcal{H}_n, \quad (4.24)$$

with the 5-dimensional effective Schrödinger potential

$$V_{\mathcal{H}} = \frac{(2S-1)A_s'' + \frac{2S-1}{z^2} - p\Phi''}{2} + \frac{\left[(2S-1)A_s' - \frac{2S-1}{z} - p\Phi'\right]^2}{4} + \frac{1}{z^2} e^{2A_s} e^{-c_{r.m.}\Phi} M_{\mathcal{H},5}^2. \quad (4.25)$$

4.3 Numerical results of glueballs/oddballs spectra

We calculate the glueballs spectra using five different holographic models defined in last section. We list the parameters used for calculating the glueballs spectra below.

4.3.1 Model I and II

In model I and model II, we choose the parameter $a = 0.6032\text{GeV}^2$. Firstly, we don't consider the distinction between glueballs (oddballs) with different P-parity and don't introduce z dependent modified 5-dimensional masses, that means $p = 1$ for even and odd parity, and $c_{r.m.} = 0$. Then we calculate the glueballs/oddballs mass spectra in model I and II, which is denoted by "Model I,II(O)" in Tab. 2. We find the calculation results of the masses of glueballs/oddballs, of which the 5D mass square M_5^2 in Tab. 1 are large, are much heavier than the lattice data, as we mentioned in subsection 4.3.1. That's why we introduce a z -dependent modified 5-dimensional mass of glueball/oddball fields in Eq. (4.4). The value of the constant $c_{r.m.}$ in Eq. (4.4) is chosen as $\frac{3}{5}$, which means

$$M_5^2(z) = e^{-\frac{3}{5}\Phi} M_5^2, \quad \text{model I, and II.} \quad (4.26)$$

The results of glueballs/oddballs spectra are denoted by "Model I,II" in Tab. 3.

Note that the 5-dimensional field Φ and ϕ are different, the relationship between them is Eq. (2.7):

$$\phi = \sqrt{\frac{8}{3}}\Phi.$$

4.3.2 Model III and IV

In model III and model IV, we choose the parameter $b = 1.760\text{GeV}^2$. The value of the constant $c_{r.m.}$ in Eq. (4.4) is chosen as $\frac{1}{2}$, which means

$$M_5(z)^2 = e^{-\frac{1}{2}\Phi} M_5^2, \quad \text{model III and IV.} \quad (4.27)$$

The results of glueballs/oddballs spectra is denoted as "Model III,IV(1)" in Tab. 3.

In Ref. [136], the authors also use model III to calculate the glueballs spectra. There they use the parameter $b = \frac{2\sqrt{6}}{3}\text{GeV}^2$ ² and $c_{r.m.} = \frac{2}{3}$. We also calculate the glueballs spectra using these parameters and list the results denoted by "Model III,IV(2)" in the Tab. 3.

²Please remember Eq. (2.7). This value of b means

$$\Phi(z) = (1\text{GeV}^2) z^2. \quad (4.28)$$

4.3.3 Model V

In model V, we choose the parameter $d = 0.2\text{GeV}^2$. The value of the constant $c_{\text{r.m.}}$ in Eq. (4.4) is chosen as $\frac{1}{3}$, which means

$$M_5(z)^2 = e^{-\frac{1}{3}\Phi} M_5^2, \quad \text{model V.} \quad (4.29)$$

The results are denoted by "Model V" in Tab. 3.

The corresponding results for glueballs and oddballs spectra are also shown in Fig. 2 and Fig. 3, respectively.

4.3.4 Compare results with lattice QCD, QCD sum rule and pp high energy scattering

We summarize our holographic results of glueballs/oddballs spectra and then compare them with the results from lattice simulation and QCD sum rule in Tab. 3. To explicitly see the difference between results from holographic QCD models and those from lattice simulation, we also list results in Fig. 2 for C-even glueballs, and in Fig. 3 for C-odd oddballs.

J^{PC}	LQCD1	LQCD2	LQCD3	LQCD4	QCDSR	Model I,II(O)
0^{++}	1.653(26)	1.475(30)(65)	1.710(50)(80)	1.730 (50) (80)	1.50 ± 0.19	2.099
0^{*++}	2.842(40)	2.755(70)(120)	—	2.670 (180)(130)	$2.0 - 2.1$	2.842
0^{***++}	—	3.370(100)(150)	—	—	—	3.425
0^{****++}	—	3.990(210)(180)	—	—	—	3.922
2^{++}	2.376(32)	2.150(30)(100)	2.390(30)(120)	2.400 (25) (120)	2.0 ± 0.1	8.831
2^{*++}	3.30(5)	2.880(100)(130)	—	—	$2.2 - 2.3$	9.515
0^{-+}	2.561(40)	2.250(60)(100)	2.560(35)(120)	2.590 (40) (130)	2.05 ± 0.19	2.099
0^{*-+}	3.54(8)	3.370(150)(150)	—	3.640 (60) (180)	$2.1 - 2.3$	2.842
1^{-+}	4.12(8)	—	—	—	—	20.675
1^{*-+}	4.16(8)	—	—	—	—	21.405
1^{**+}	4.20(9)	—	—	—	—	22.093
2^{-+}	3.07(6)	2.780(50)(130)	3.040(40)(150)	3.100 (30) (150)	—	8.831
2^{*-+}	3.97(7)	3.480(140)(160)	—	3.890 (40) (190)	—	9.515
0^{+-}	—	—	4.780(60)(230)	4.740 (70) (230)	$9.2^{+1.3}_{-1.4}$	28.137
1^{+-}	2.944(42)	2.670(65)(120)	2.980(30)(140)	2.940 (30) (140)	$2.87^{+0.17}_{-0.20}$	16.457
1^{*+-}	3.80(6)	—	—	—	—	17.176
2^{+-}	4.24(8)	—	4.230(50)(200)	4.140 (50) (200)	$2.85^{+0.16}_{-0.20}$ 6.06 ± 0.13	16.996
3^{+-}	3.53(8)	3.270(90)(150)	3.600(40)(170)	3.550 (40) (170)	$2.78^{+0.18}_{-0.23}$	16.491
3^{*+-}	—	3.630(140)(160)	—	—	—	17.212
0^{--}	—	—	—	—	$6.8^{+1.1}_{-1.2}$	28.137
1^{--}	4.03(7)	3.240(330)(150)	3.830(40)(190)	3.850 (50) (190)	$3.29^{+1.49}_{-0.32}$	16.457
2^{--}	3.92(9)	3.660(130)(170)	4.010(45)(200)	3.930 (40) (190)	$3.16^{+0.33}_{-0.23}$	16.996
2^{*-}	—	3.740(200)(170)	—	—	—	17.717
3^{--}	—	4.330(260)(200)	4.200(45)(200)	4.130 (90) (200)	$3.47^{+?}_{-0.50}$	16.491

Table 2. The glueballs and oddballs mass spectra in the dynamical soft-wall model I and II without making a distinction between glueballs (oddballs) with different P -parity and introducing z dependent modified 5-dimensional masses, compared with results from lattice QCD and QCD sum rule. The units of all the data in the table are GeV. The lattice data in the column "LQCD1", column "LQCD2", column "LQCD3", and column "LQCD4" are taken from Ref. [9], Ref [4], Ref [5], and Ref [2] respectively. The QCD sum rule results are take from Refs. [22, 27, 31, 32]. Here we also list the data predicted by the single pole (SP) and dipole (DP) Regge model [52]: using the SP Regge model, the predicted mass for 2^{++} glueball is 1.747GeV; using the DP Regge model, the predicted masses for 2^{++} glueball and 3^{--} oddball are 1.758GeV and 3.001GeV respectively.

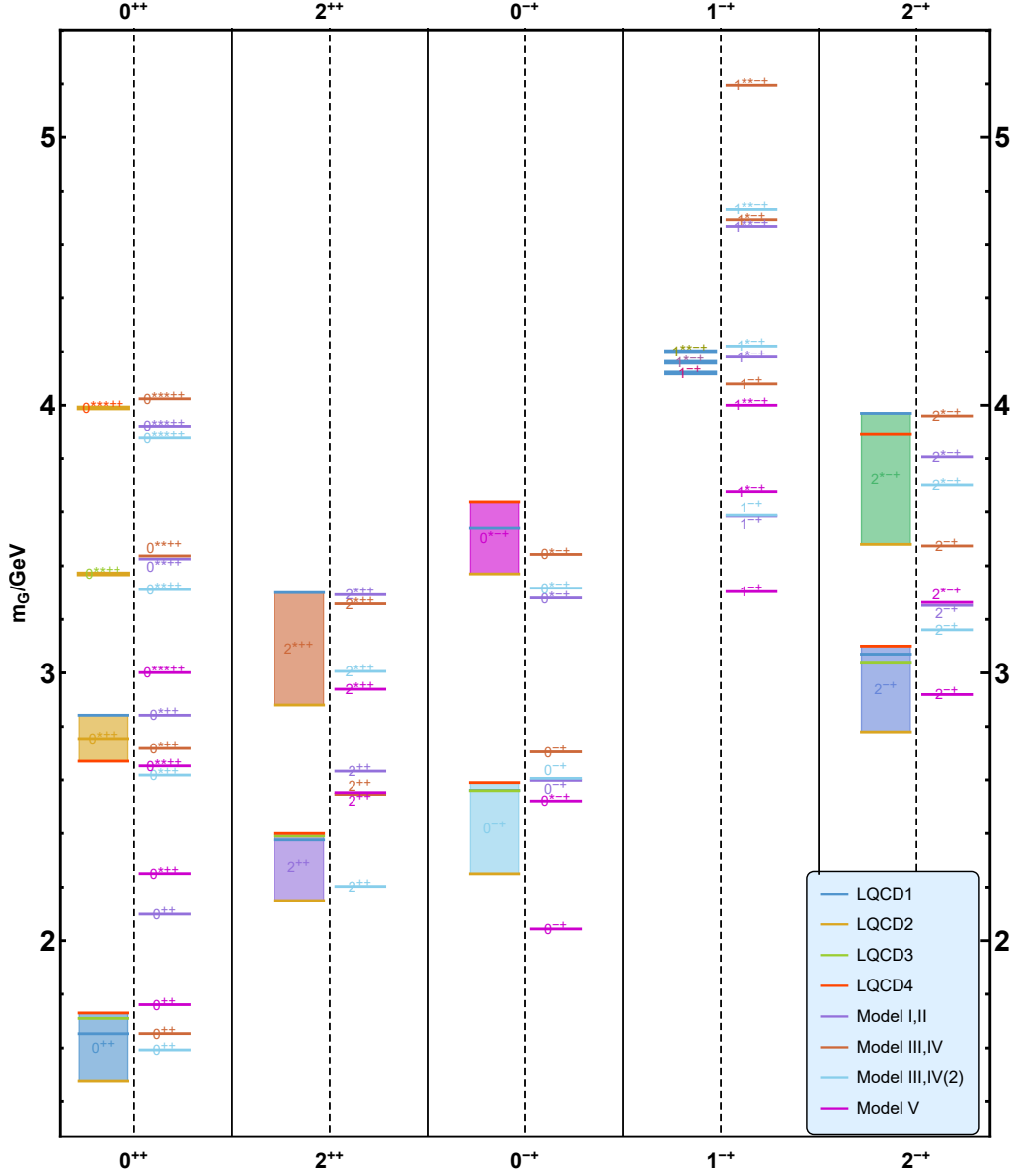


Figure 2. The mass spectra of J^{PC} ($C = 1$) glueballs in the dynamical soft-wall model, compared with lattice data. This figure are split into five panels, that are divided by black solid lines. From left to right, the mass data in these panels belong to 0^{++} states, 2^{++} states, 0^{-+} states, 1^{-+} states, and 2^{-+} states respectively. In every panel, the black dashed line split it into two parts. The left one contains lattice data taken from Refs. [2, 4, 5, 9]. The steel blue lines, goldenrod lines, olive drab lines, orange red lines are lattice data taken from Ref. [9], Ref [4], Ref [5], and Ref [2] respectively. The minimal value and maximal value of a set of discrete data that belongs to the same glueball state decide the positions of lower and upper bound of the bar in the figure respectively. The data in the right part are calculated in our holographic models. The medium purple lines, sienna lines, sky blue lines, and magenta lines are results from "Model I,II", "Model III,IV(1)", "Model III,IV(2)", and "Model V" respectively.

J^{PC}	LQCD1-4	QCDSR	Model I,II	Model III,IV(1)	Model III,IV(2)	Model V
0^{++}	1.475(30)(65) - 1.730(50)(80)	1.50 ± 0.19	2.099	1.653	1.593	1.761
0^{*++}	2.670 (180)(130) - 2.842(40)	$2.0 - 2.1$	2.842	2.718	2.618	2.251
0^{***++}	3.370(100)(150)	—	3.425	3.437	3.311	2.653
0^{****++}	3.990(210)(180)	—	3.922	4.024	3.877	3.001
2^{++}	2.150(30)(100) - 2.400(25)(120)	2.0 ± 0.1	2.633	2.546	2.203	2.553
2^{*++}	2.880(100)(130) - 3.30(5)	$2.2 - 2.3$	3.292	3.258	3.006	2.939
0^{-+}	2.250(60)(100) - 2.590(40)(130)	2.05 ± 0.19	2.599	2.705	2.606	2.043
0^{*-+}	3.370(150)(150) - 3.640(60)(180)	$2.1 - 2.3$	3.280	3.443	3.317	2.522
1^{-+}	4.12(8)	—	3.585	4.079	3.588	3.304
1^{*-+}	4.16(8)	—	4.180	4.692	4.221	3.678
1^{**+}	4.20(9)	—	4.667	5.195	4.730	4.000
2^{-+}	2.780(50)(130) - 3.100(30)(150)	—	3.252	3.474	3.161	2.919
2^{*-+}	3.480(140)(160) - 3.97(7)	—	3.806	3.960	3.703	3.263
0^{+-}	4.740 (70) (230) - 4.780(60)(230)	$9.2^{+1.3}_{-1.4}$	3.268	3.742	3.165	3.184
1^{+-}	2.670(65)(120) - 2.980(30)(140)	$2.87^{+0.17}_{-0.20}$	3.114	3.448	2.954	2.982
1^{*+-}	3.80(6)	—	3.755	4.099	3.652	3.373
2^{+-}	4.140 (50) (200) - 4.24(8)	$2.85^{+0.16}_{-0.20},$ 6.06 ± 0.13	3.002	3.303	2.786	2.926
3^{+-}	3.270(90)(150) - 3.600(40)(170)	$2.78^{+0.18}_{-0.23}$	2.857	3.100	2.572	2.837
3^{*+-}	3.630(140)(160)	—	3.542	3.818	3.369	3.244
0^{--}	—	$6.8^{+1.1}_{-1.2}$	3.843	4.426	3.907	3.514
1^{--}	3.240(330)(150) - 4.03(7)	$3.29^{+1.49}_{-0.32}$	3.470	3.901	3.441	3.190
2^{--}	3.660(130)(170) - 4.010(45)(200)	$3.16^{+0.33}_{-0.23}$	3.602	4.073	3.619	3.273
2^{*-}	3.740(200)(170)	—	4.177	4.645	4.211	3.637
3^{--}	4.130(90)(200) - 4.330(260)(200)	$3.47^{+?}_{-0.50}$	3.705	4.201	3.765	3.326

Table 3. The glueballs and oddballs mass spectra in the dynamical soft-wall model, compared with results from lattice QCD and QCD sum rule. The units of all the data in the table are GeV. The lattice data are taken from Refs. [2, 4, 5, 9]. The QCD sum rule results are take from Refs. [22, 27, 31, 32]. Here we also list the data predicted by the SP and DP Regge model [52]: using the SP Regge model, the predicted mass for 2^{++} glueball is 1.747GeV; using the DP Regge model, the predicted masses for 2^{++} glueball and 3^{--} oddball are 1.758GeV and 3.001GeV respectively.

In the framework of holography, the states J^{PC} with the same angular momentum J and the same C-parity share the same operator. Thus, they have the same dimension and 5-dimensional mass, and the mass splitting for different P-parity states is realized by $e^{-p\Phi}$ in Eq. (4.1). The states J^{PC} with the same angular momentum J and the same P-parity but different C-parity have different operators. Thus, they have different 5-dimensional masses, which naturally induces the mass splitting for different C-parity states. From the results in Table 3, Fig.2, and Fig. 3, we can see that with only 2 parameters, the model predictions on glueballs/oddballs spectra in general are in good agreement with lattice results except two oddballs 0^{+-} and 2^{+-} . Here we also would like to mention that the data predicted by the single pole (SP) and dipole (DP) Regge model [52] to fit the high energy pp scattering: using the SP Regge model, the predicted mass for 2^{++} glueball is 1.747GeV; using the DP Regge model, the predicted masses for 2^{++} glueball and 3^{--} oddball are 1.758GeV and 3.001GeV respectively. These predicted values are a little bit lower than the results predicted from holography but still in reasonable regions. It might indicate that the mass 1.747GeV/1.758GeV 2^{++} glueball and mass 3.001GeV 3^{--} oddball are hybrid glueball/oddball states mixing with quark states.

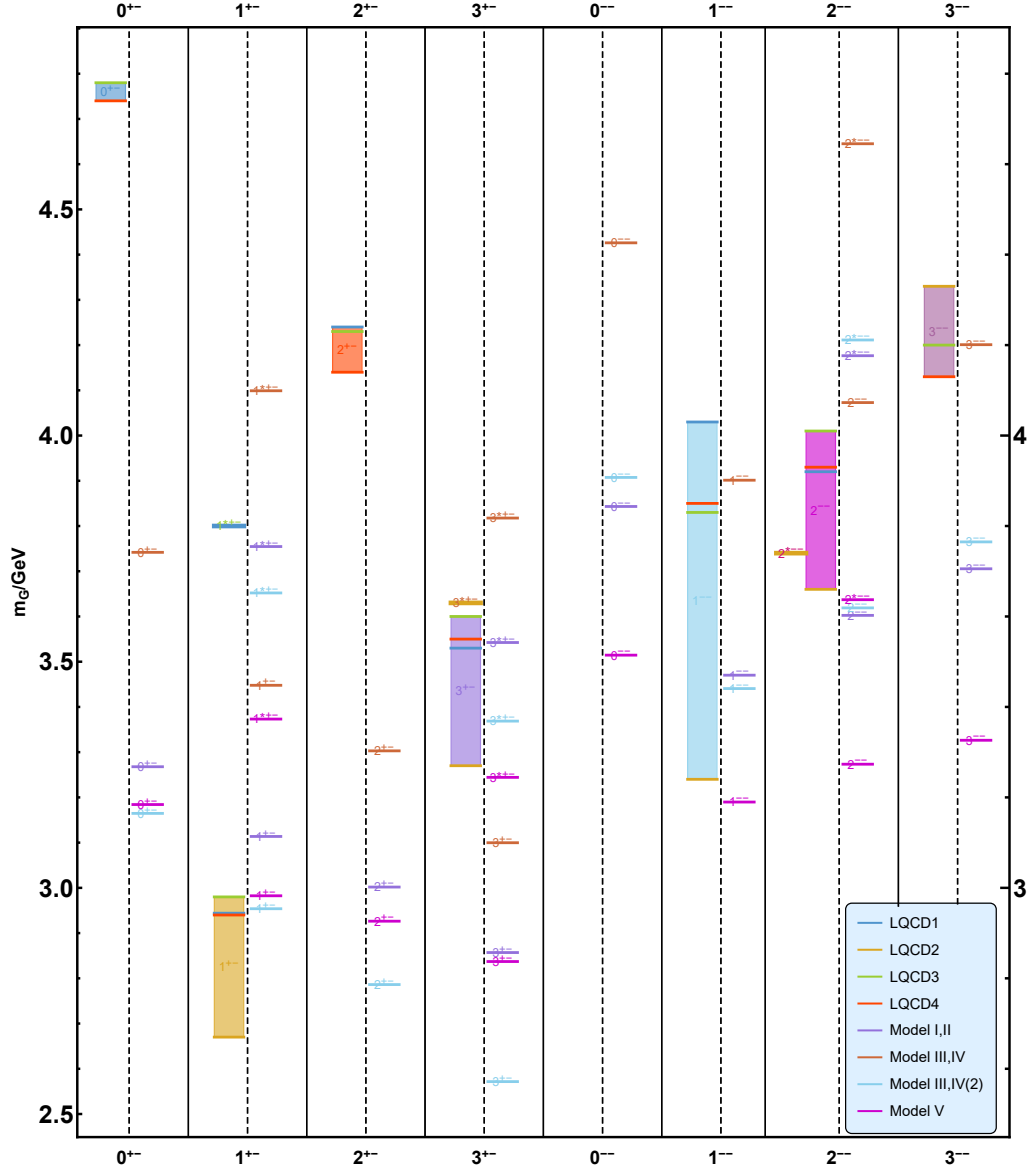


Figure 3. The mass spectra of J^{PC} ($C = -1$) oddballs in the dynamical soft-wall model, compared with lattice data. This figure are split into eight panels, that are divided by black solid lines. From left to right, the mass data in these panels belong to 0^{+-} states, 1^{+-} states, 2^{+-} states, 3^{+-} states, 0^{-+} states, 1^{-+} states, 2^{-+} states, and 3^{-+} states respectively. In every panel, the black dashed line split it into two parts. The left one contains lattice data taken from Refs. [2, 4, 5, 9]. The steel blue lines, goldenrod lines, olive drab lines, orange red lines are lattice data taken from Ref. [9], Ref [4], Ref [5], and Ref [2] respectively. The minimal value and maximal value of a set of discrete data that belongs to the same oddball state decide the positions of lower and upper bound of the bar in the figure respectively. The data in the right part are calculated in our holographic models. The medium purple lines, sienna lines, sky blue lines, and magenta lines are results from "Model I,II", "Model III,IV(1)", "Model III,IV(2)", and "Model V" respectively.

5 Equation of state

With parameters used to calculate the glueballs/oddballs spectra listed in Table 3, we check the corresponding thermodynamical properties of the system.

5.1 Model I and II

In Model I and Model II, we choose the parameter $a = 0.6032\text{GeV}^2$, the 5-dimensional Newton constant $G_5 = 1$. Then we numerically calculate the thermodynamical properties for Model I and II. In model II, we utilize the numerical method in Refs. [126, 137] to investigate the thermodynamical properties. The results are different for these two models, as we emphasized in subsubsection 3.3.1. The deconfined temperature $T_c = 537.960\text{MeV}$ for model I with inputting $A_E(z)$ and $T_c = 521.147\text{MeV}$ for model II with inputting $V_\phi(\phi)$. We plot the thermodynamical quantities in Fig. 4. The red points with error bar is lattice simulation of $SU(3)$ Yang-Mills results in Ref. [138].

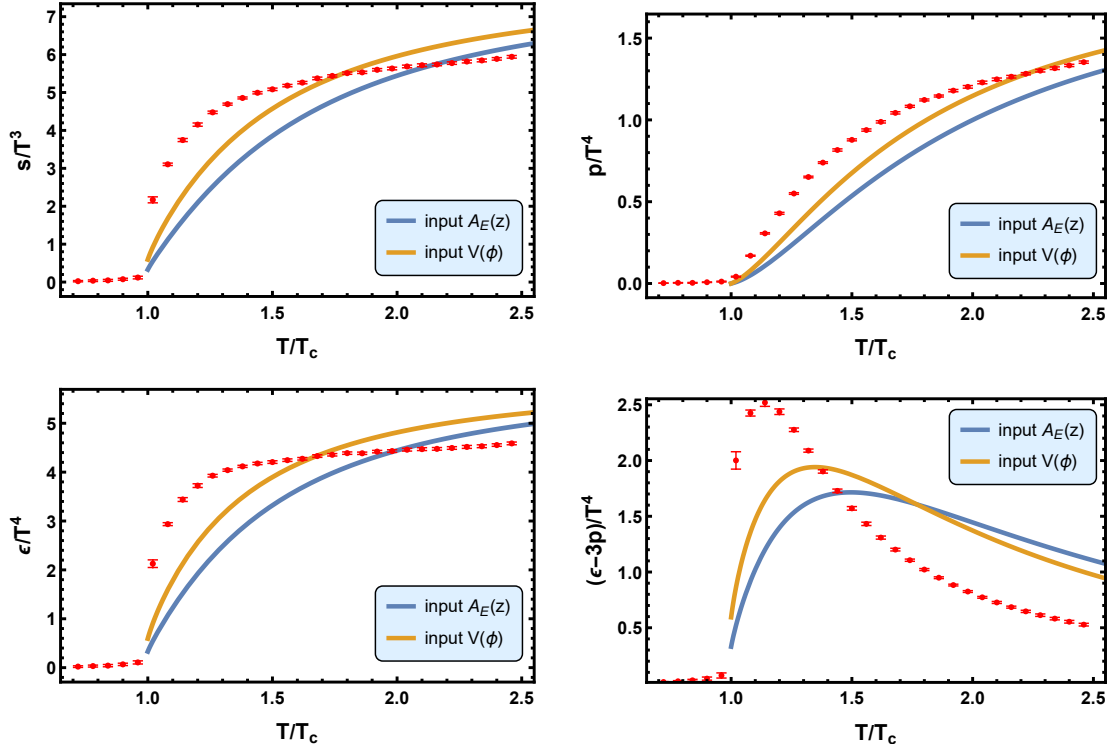


Figure 4. The results of equation of state from model I and model II with $a = 0.6032\text{GeV}^2$ and $G_5 = 1$. The results of the entropy density over cubic temperature (upper left panel), the pressure density over quartic temperature (upper right panel), the energy density over quartic temperature (lower left panel) and the trace anomaly over quartic temperature (lower right panel) as functions of the scaled temperature T/T_c in model I and model II, respectively. The blue line is the result for model I with inputting $A_E(z)$, the orange line is result for model II with inputting $V_\phi(\phi)$. The red points are $SU(3)$ lattice data taken from Ref. [138].

It is noticed that even though Model I and Model II can describe glueballs/oddballs spectra, the corresponding thermodynamical properties shown in Fig. 4 are not in good agreement with lattice results [138] for the pure gluon system. From the asymptotic analysis of the dilaton field at UV boundary Eq. (3.9) in subsection 3.1, we can see that the leading order of the 5-dimensional dilaton field is a term proportional to z , and the sub-leading order is a term proportional to z^3 . So we expect the thermodynamical properties of model I and II behaves more like quark matter. We fix the value of the parameter a , and tune the value of $G_5 = 1$ to $G_5 = 0.42$ to meet the degrees of freedom of quark matter. In this case, the critical temperatures remain unchanged. It is found that the equation of state calculated in model I and II are qualitatively consistent with the $2+1$ flavors lattice results in Ref. [139]. We plot the equation of state in Fig. 5. The red points with error bar is lattice simulation of $SU(3)$ equation of state taken from Ref. [138] for pure gluon system. The purple points with error bar is lattice simulation of $N_f = 2+1$ QCD equation of state taken from Ref. [139].

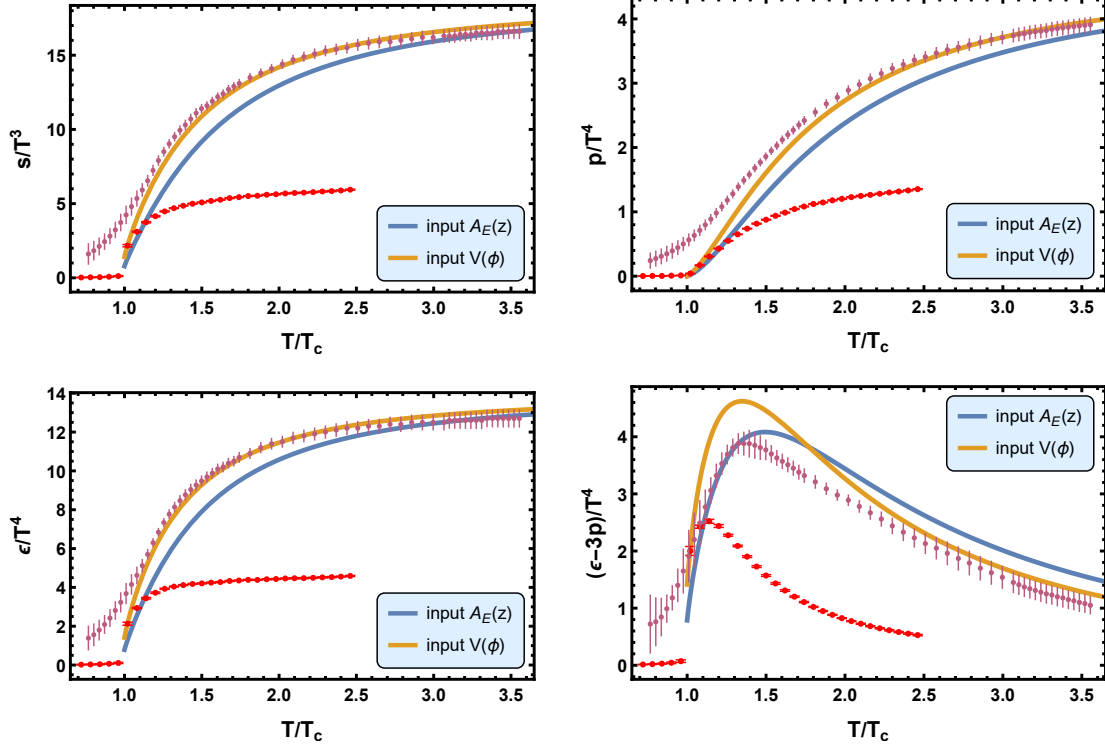


Figure 5. The results of equation of state from model I and model II with $a = 0.6032\text{GeV}^2$ and $G_5 = 0.42$. Upper left panel: The ratio of entropy density over cubic temperature as function of scaled temperature T/T_c . Upper right panel: The ratio of pressure density over quartic temperature as function of scaled temperature T/T_c . Lower left panel: The energy density over quartic temperature as function of scaled temperature T/T_c . Lower right panel: The trace anomaly over quartic temperature as function of scaled temperature T/T_c . The blue line is for model I with inputting $A_E(z)$. The orange line is for model II with inputting $V_\phi(\phi)$. The red points are $SU(3)$ lattice data taken from Ref. [138], and the purple points are $N_f = 2 + 1$ lattice data taken from Ref. [139].

5.2 Model III and IV

We also check the corresponding thermodynamical properties of Model III and IV. In model III, we choose two sets of parameters. The parameters I are $b = 1.760\text{GeV}^2$, and the 5-dimensional Newtown constant $G_5 = 1.35$; the parameters II are $b = \frac{2\sqrt{6}}{3}\text{GeV}^2$ as in [136], as we mention in subsubsection 4.3.2, the 5-dimensional Newtown constant $G_5 = 1.35$. Again, we employ the numerical method in Refs. [126, 137] to investigate the thermodynamical propertities for model IV. Then we fix the values of the characteristic energy scale³ of the EMD system Λ and the 5-dimensional Newtown constant G_5 : $\Lambda = 1\text{GeV}$, and $G_5 = 1.35$. Then we numerically calculate the equation of state for these two models respectively. The results are actually different for the two models, as we emphasized in subsubsection

³As explained in Ref. [137], the characteristic energy scale Λ , the energy dimension of which is 1, is introduced to express dimensionful observables in physical unit. When an gauge/gravity observable with dimension $[E]^q$ is expressed in physical unit, it should be multiplied by Λ^q .

3.3.2. In model III, the deconfined temperature $T_c = 367.597\text{MeV}$ for parameters I with $b = 1.760\text{GeV}^2$ and $T_c = 354.131\text{MeV}$ for parameters II with $b = \frac{2\sqrt{6}}{3}\text{GeV}^2$. The deconfined temperature $T_c = 269.371\text{MeV}$ in model IV with $\Lambda = 1\text{GeV}$. We plot the equation of state in Fig. 6. The red points with error bar is lattice simulation of $SU(3)$ equation of state for pure gluon system in Ref. [138].

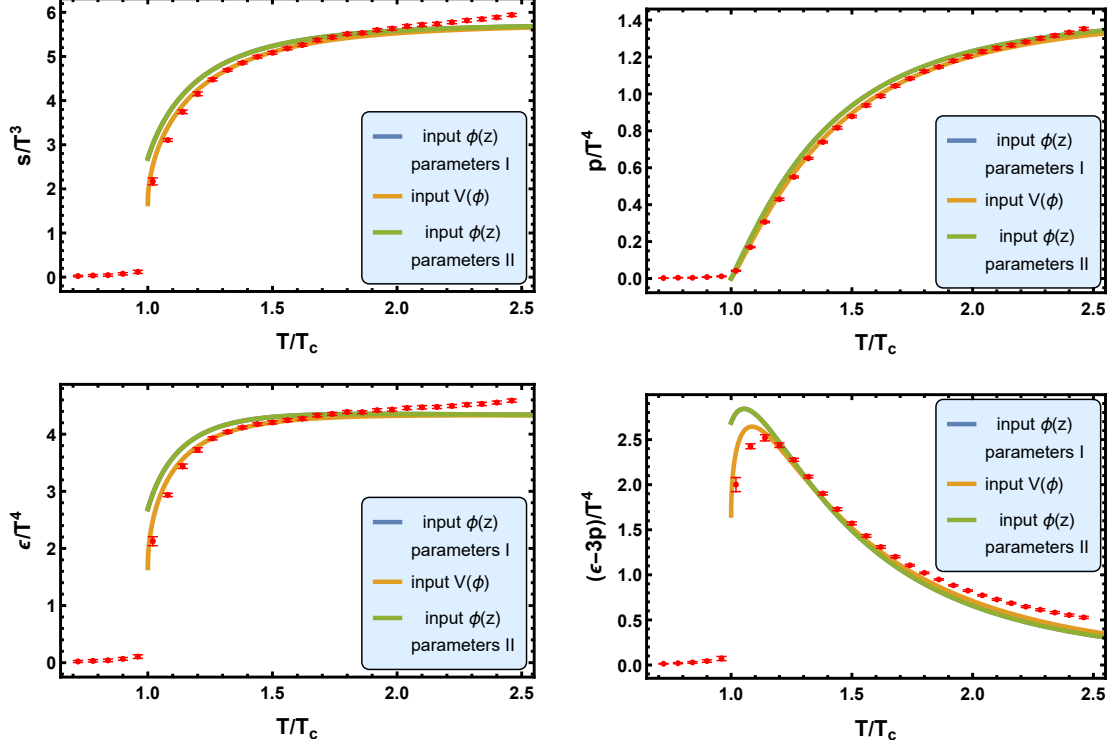


Figure 6. The results of equation of state from model III and model IV. Upper left panel: The ratio of entropy density over cubic temperature as function of scaled temperature T/T_c . Upper right panel: The ratio of pressure density over quartic temperature as function of scaled temperature T/T_c . Lower left panel: The energy density over quartic temperature as function of scaled temperature T/T_c . Lower right panel: The trace anomaly over over quartic temperature as function of scaled temperature T/T_c . The blue line is for parameters I: $b = 1.760\text{GeV}^2$, and $G_5 = 1.35$ in model III, in which we input $\phi(z)$. The green line is for parameters II: $b = \frac{2\sqrt{6}}{3}\text{GeV}^2$, and $G_5 = 1.35$ in model III. The orange line is for model IV, in which we input $V_\phi(\phi)$ and the parameters are $\Lambda = 1\text{GeV}$, and $G_5 = 1.35$. The red points is $SU(3)$ lattice data taken from Ref. [138] for pure gluon system. The positions of the blue line and the green line are totally the same in each panel.

We can see from the Fig. 6 that the lines from parameters I and parameters II in model III are totally the same with each other. That is not surprising because all the quantities are dimensionless in this plot.

5.3 Model V

In Model V, we take the parameter $d = 0.2\text{GeV}^2$, and the 5-dimensional Newton constant $G_5 = \frac{10}{11}$. Then we numerically calculate the equation of state. The deconfined temperature $T_c = 470.833\text{MeV}$. We plot the equation of state in Fig. 7. The red points with error bar is lattice simulation of $SU(3)$ equation of state from Ref. [138].

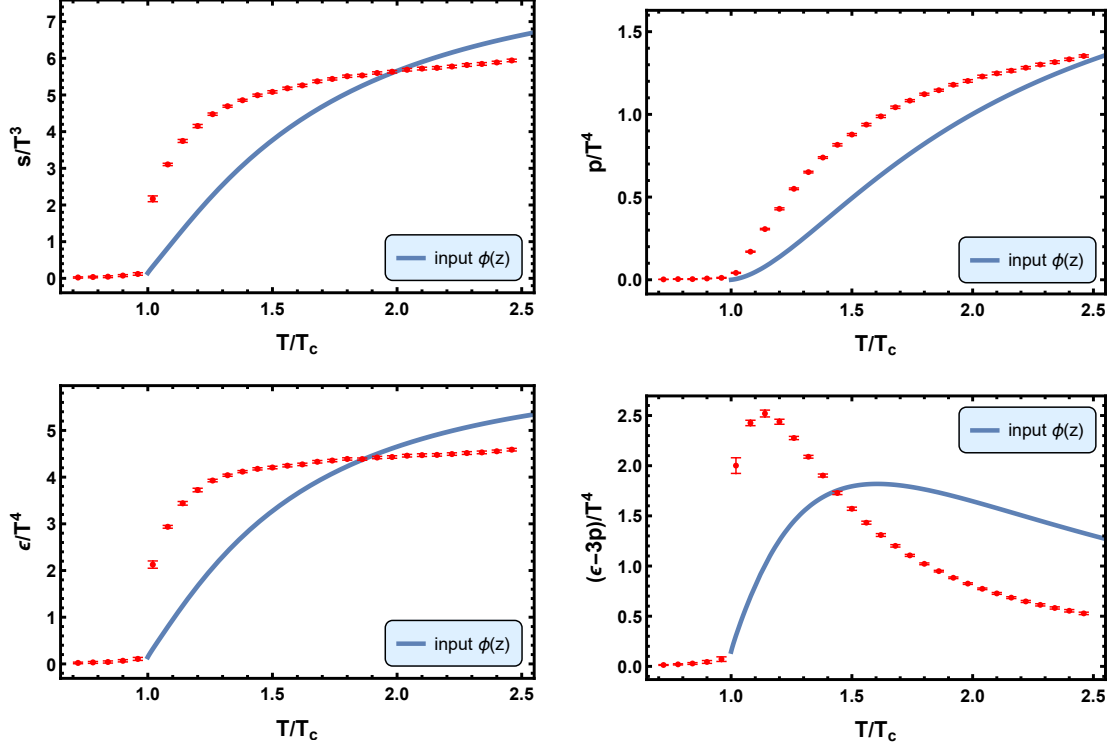


Figure 7. The results of equation of state from model V. Upper left panel: The ratio of entropy density over cubic temperature as function of scaled temperature T/T_c . Upper right panel: The ratio of pressure density over quartic temperature as function of scaled temperature T/T_c . Lower left panel: The energy density over quartic temperature as function of scaled temperature T/T_c . Lower right panel: The trace anomaly over over quartic temperature as function of scaled temperature T/T_c . The blue line is for Model V, in which we input $\phi(z)$ and the parameters are $d = 0.2\text{GeV}^2$, and $G_5 = \frac{10}{11}$. The red points are $SU(3)$ lattice data taken from Ref. [138] for pure gluon system.

If we fix the value of the parameter d and tune the value of G_5 to $G_5 = 0.39$, the critical temperature remains unchanged. However, the equation of state in Model V will be qualitatively consistent with the $2 + 1$ flavors lattice results, which is taken from Ref. [139]. We plot the equation of state in Fig. 8. The red points with error bar is lattice simulation of $SU(3)$ equation of state taken from Ref. [138]. The purple points with error bar is lattice simulation of $N_f = 2 + 1$ QCD equation of state taken from Ref. [139].

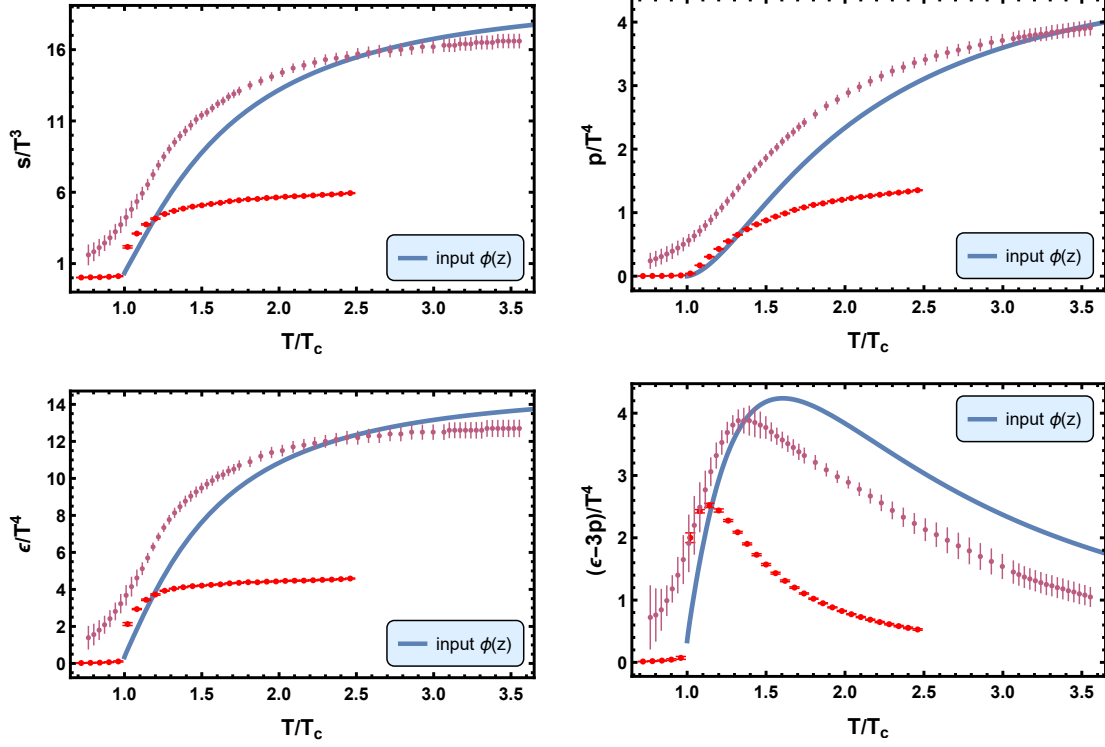


Figure 8. The results of equation of state from model V. Upper left panel: The ratio of entropy density over cubic temperature as function of scaled temperature T/T_c . Upper right panel: The ratio of pressure density over quartic temperature as function of scaled temperature T/T_c . Lower left panel: The energy density over quartic temperature as function of scaled temperature T/T_c . Lower right panel: The trace anomaly over over quartic temperature as function of scaled temperature T/T_c . The blue line is for Model V, in which we input $\phi(z)$. The blue line is theoretical result from model V, in which we input $\phi(z)$ and the parameters are $d = 0.2\text{GeV}^2$, and $G_5 = 0.39$. The red points are $SU(3)$ lattice data taken from Ref. [138] for pure gluon system, and the purple points are $N_f = 2 + 1$ lattice data taken from Ref. [139].

6 Conclusion and discussion

In this work, we study scalar, vector and tensor glueballs/oddballs spectra in the framework of 5-dimensional dynamical holographic QCD model, where the metric structure is deformed self-consistently by the dilaton field. In the framework of holography, the states J^{PC} with the same angular momentum J and the same C-parity share the same operator thus have the same dimension and 5-dimensional mass, and the mass splitting for different P-parity states is realized by $e^{-p\Phi}$ in Eq. (4.1). The states J^{PC} with the same angular momentum J and the same P-parity but different C-parity have different operators. Thus, they have different 5-dimensional masses, which naturally induces the mass splitting for different C-parity states.

From the results in Table 3, Fig. 2, and Fig. 3, we can see that with only 2 parameters, the model predictions on glueballs/oddballs spectra in general are in good agreement with lattice results except two oddballs 0^{+-} and 2^{+-} . Here we also would like to mention

that the data predicted by the SP and DP Regge model [52] to fit the high energy pp scattering: using the SP Regge model, the predicted mass for 2^{++} glueball is 1.747GeV; using the DP Regge model, the predicted masses for 2^{++} glueball and 3^{--} oddball are 1.758GeV and 3.001GeV respectively. These predicted values are a little bit lower than the results predicted from holography but still in reasonable regions. It might indicate that the mass 1.747GeV/1.758GeV 2^{++} glueball and mass 3.001GeV 3^{--} oddball are hybrid glueball/oddball states mixing with quark states.

From the results of glueballs/oddballs spectra at zero temperature and zero density and the equation of state at finite temperature, we obtain the following conclusions. 1) For the same set of vacuum solutions for the Einstein field equations and the equation of motion of the dilaton field $\phi(z)$, inputting the function $A_E(z)$ and inputting the dilaton potential $V_\phi(\phi)$ give different equation of state indeed. The difference between Model III and IV are much less than that between Model I and II. 2) The model with quadratic dilaton field $\phi(z)$ can simultaneously describe glueballs/oddballs spectra as well as equation of state of pure gluon system. The model with quadratic $A_E(z)$ can describe glueballs/oddballs spectra, but its corresponding equation of state behaves more like $N_f = 2 + 1$ quark matter. These are consistent with dimension analysis at UV boundary.

Acknowledgement

We thank Danning Li and Cong-Feng Qiao for helpful discussions. This work is supported in part by the National Natural Science Foundation of China (NSFC) Grant Nos. 11735007, 11725523, and Chinese Academy of Sciences under Grant No. XDPB09, the start-up funding from University of Chinese Academy of Sciences(UCAS), and the Fundamental Research Funds for the Central Universities.

References

- [1] M. Gell-Mann. Quarks. *Acta Phys. Austriaca Suppl.*, 9:733–761, 1972.
- [2] Colin J. Morningstar and Mike J. Peardon. The Glueball spectrum from an anisotropic lattice study. *Phys. Rev. D*, 60:034509, 1999.
- [3] B. Lucini and M. Teper. SU(N) gauge theories in four-dimensions: Exploring the approach to $N = \infty$. *JHEP*, 06:050, 2001.
- [4] Harvey B. Meyer. Glueball regge trajectories. Other thesis, 2004.
- [5] Y. Chen et al. Glueball spectrum and matrix elements on anisotropic lattices. *Phys. Rev. D*, 73:014516, 2006.
- [6] E. Gregory, A. Irving, B. Lucini, C. McNeile, A. Rago, C. Richards, and E. Rinaldi. Towards the glueball spectrum from unquenched lattice QCD. *JHEP*, 10:170, 2012.
- [7] Ed Bennett, Deog Ki Hong, Jong-Wan Lee, C. J. David Lin, Biagio Lucini, Maurizio Piai, and Davide Vadacchino. Sp(4) gauge theory on the lattice: towards SU(4)/Sp(4) composite Higgs (and beyond). *JHEP*, 03:185, 2018.
- [8] Ed Bennett, Jack Holligan, Deog Ki Hong, Jong-Wan Lee, C. J. David Lin, Biagio Lucini, Maurizio Piai, and Davide Vadacchino. Color dependence of tensor and scalar glueball masses in Yang-Mills theories. *Phys. Rev. D*, 102(1):011501, 2020.
- [9] Andreas Athenodorou and Michael Teper. The glueball spectrum of SU(3) gauge theory in $3 + 1$ dimensions. *JHEP*, 11:172, 2020.
- [10] Ed Bennett, Jack Holligan, Deog Ki Hong, Jong-Wan Lee, C. J. David Lin, Biagio Lucini, Maurizio Piai, and Davide Vadacchino. Glueballs and strings in $Sp(2N)$ Yang-Mills theories. *Phys. Rev. D*, 103(5):054509, 2021.
- [11] Andreas Athenodorou and Michael Teper. SU(N) gauge theories in $3+1$ dimensions: glueball spectrum, string tensions and topology. 6 2021.
- [12] Nathan Isgur and Jack E. Paton. A Flux Tube Model for Hadrons in QCD. *Phys. Rev. D*, 31:2910, 1985.
- [13] R. L. Jaffe and K. Johnson. Unconventional States of Confined Quarks and Gluons. *Phys. Lett. B*, 60:201–204, 1976.
- [14] Ted Barnes, F. E. Close, and S. Monaghan. Hyperfine Splittings of Bag Model Gluonia. *Nucl. Phys. B*, 198:380–406, 1982.
- [15] Ted Barnes, F. E. Close, and S. Monaghan. The MIT Bag Can Accomodate the $\theta(1640)$ and Iota (1440) as Glueballs. *Phys. Lett. B*, 110:159–161, 1982.
- [16] C. E. Carlson, T. H. Hansson, and C. Peterson. Meson, Baryon and Glueball Masses in the MIT Bag Model. *Phys. Rev. D*, 27:1556–1564, 1983.
- [17] Michael S. Chanowitz and Stephen R. Sharpe. Hybrids: Mixed States of Quarks and Gluons. *Nucl. Phys. B*, 222:211–244, 1983. [Erratum: Nucl.Phys.B 228, 588–588 (1983)].
- [18] C. A. Dominguez and N. Paver. LOCAL DUALITY CONSTRAINTS ON SCALAR GLUONIUM. *Z. Phys. C*, 31:591, 1986.
- [19] C. A. Dominguez and N. Paver. Tensor Gluonium Spectrum in QCD. *Z. Phys. C*, 32:391, 1986.

- [20] J. I. Latorre, Stephan Narison, and S. Paban. 0^{++} TRIGLUONIUM SUM RULES. *Phys. Lett. B*, 191:437–441, 1987.
- [21] Stephan Narison and G. Veneziano. QCD Tests of $G(1.6) = \text{Glueball}$. *Int. J. Mod. Phys. A*, 4:2751, 1989.
- [22] Stephan Narison. Masses, decays and mixings of gluonia in QCD. *Nucl. Phys. B*, 509:312–356, 1998.
- [23] Stephan Narison. Masses, decays and mixings of gluonia in QCD. *Nucl. Phys. B Proc. Suppl.*, 64:210–219, 1998.
- [24] Tao Huang, Hong-Ying Jin, and Ai-Lin Zhang. Determination of the scalar glueball mass in QCD sum rules. *Phys. Rev. D*, 59:034026, 1999.
- [25] Stephan Narison. Light scalar mesons in QCD. *Nucl. Phys. B Proc. Suppl.*, 186:306–311, 2009.
- [26] Cong-Feng Qiao and Liang Tang. Finding the 0^{--} Glueball. *Phys. Rev. Lett.*, 113(22):221601, 2014.
- [27] Liang Tang and Cong-Feng Qiao. Mass spectra of 0^{+-} , 1^{-+} , and 2^{+-} exotic glueballs. *Nucl. Phys. B*, 904:282–296, 2016.
- [28] Alexandr Pimikov, Hee-Jung Lee, Nikolai Kochelev, and Pengming Zhang. Is the exotic 0^{--} glueball a pure gluon state ? *Phys. Rev. D*, 95(7):071501, 2017.
- [29] Alexandr Pimikov, Hee-Jung Lee, and Nikolai Kochelev. Comment on "Finding the 0^{--} Glueball". *Phys. Rev. Lett.*, 119(7):079101, 2017.
- [30] Cong-Feng Qiao and Liang Tang. Reply to "Comment on 'Finding the 0^{--} Glueball'" [arXiv:1702.06634] and comment on 'Is the exotic 0^{--} glueball a pure gluon state?' [arXiv:1611.08698]. 4 2017.
- [31] Alexandr Pimikov, Hee-Jung Lee, Nikolai Kochelev, Pengming Zhang, and Viachaslau Khandramai. Exotic glueball $0^{\pm-}$ states in QCD sum rules. *Phys. Rev. D*, 96(11):114024, 2017.
- [32] Hua-Xing Chen, Wei Chen, and Shi-Lin Zhu. Toward the existence of the odderon as a three-gluon bound state. *Phys. Rev. D*, 103(9):L091503, 2021.
- [33] Adam Szczepaniak, Eric S. Swanson, Chueng-Ryong Ji, and Stephen R. Cotanch. Glueball spectroscopy in a relativistic many body approach to hadron structure. *Phys. Rev. Lett.*, 76:2011–2014, 1996.
- [34] Felipe J. Llanes-Estrada, Stephen R. Cotanch, Pedro J. de A. Bicudo, J. Emilio F. T. Ribeiro, and Adam P. Szczepaniak. QCD glueball Regge trajectories and the Pomeron. *Nucl. Phys. A*, 710:45–54, 2002.
- [35] Felipe J. Llanes-Estrada, Pedro Bicudo, and Stephen R. Cotanch. Oddballs and a low odderon intercept. *Phys. Rev. Lett.*, 96:081601, 2006.
- [36] D. V. Bugg, Mike J. Peardon, and B. S. Zou. The Glueball spectrum. *Phys. Lett. B*, 486:49–53, 2000.
- [37] Qiang Zhao, Bing-song Zou, and Zhong-biao Ma. Glueball-Q anti-Q mixing and Okuba-Zweig-Iizuka rule violation in the hadronic decays of heavy quarkonia. *Phys. Lett. B*, 631:22–31, 2005.

- [38] Hai-Yang Cheng, Chun-Khiang Chua, and Keh-Fei Liu. Scalar glueball, scalar quarkonia, and their mixing. *Phys. Rev. D*, 74:094005, 2006.
- [39] Bing An Li. Chiral field theory of 0^{++} glueball. *Phys. Rev. D*, 81:114002, 2010.
- [40] Song He, Mei Huang, and Qi-Shu Yan. The Pseudoscalar glueball in a chiral Lagrangian model with instanton effect. *Phys. Rev. D*, 81:014003, 2010.
- [41] Hai-Yang Cheng. Scalar and Pseudoscalar Glueballs Revisited. *AIP Conf. Proc.*, 1257(1):477–481, 2010.
- [42] Stanislaus Janowski, Francesco Giacosa, and Dirk H. Rischke. Is $f_0(1710)$ a glueball? *Phys. Rev. D*, 90(11):114005, 2014.
- [43] Walaa I. Eshraim. *Phenomenology of a pseudoscalar glueball and charmed mesons*. PhD thesis, Frankfurt U., 2015.
- [44] A. V. Sarantsev, I. Denisenko, U. Thoma, and E. Klempt. Scalar isoscalar mesons and the scalar glueball from radiative J/ψ decays. *Phys. Lett. B*, 816:136227, 2021.
- [45] Vincent Mathieu, Nikolai Kochelev, and Vicente Vento. The Physics of Glueballs. *Int. J. Mod. Phys. E*, 18:1–49, 2009.
- [46] Eberhard Klempt and Alexander Zaitsev. Glueballs, Hybrids, Multiquarks. Experimental facts versus QCD inspired concepts. *Phys. Rept.*, 454:1–202, 2007.
- [47] Claude Amsler and N. A. Tornqvist. Mesons beyond the naive quark model. *Phys. Rept.*, 389:61–117, 2004.
- [48] M. A. Braun. Odderon and QCD. 5 1998.
- [49] L. Lukaszuk and B. Nicolescu. A Possible interpretation of $p p$ rising total cross-sections. *Lett. Nuovo Cim.*, 8:405–413, 1973.
- [50] Victor Mukhamedovich Abazov et al. Measurement of the differential cross section $d\sigma/dt$ in elastic $p\bar{p}$ scattering at $\sqrt{s} = 1.96$ TeV. *Phys. Rev. D*, 86:012009, 2012.
- [51] V. M. Abazov et al. Comparison of pp and $p\bar{p}$ differential elastic cross sections and observation of the exchange of a colorless C -odd gluonic compound. 12 2020.
- [52] István Szanyi, László Jenkovszky, Rainer Schicker, and Volodymyr Svintozelskyi. Pomeron/glueball and odderon/oddball trajectories. *Nucl. Phys. A*, 998:121728, 2020.
- [53] T. Csörgő, T. Novak, R. Pasechnik, A. Ster, and I. Szanyi. Evidence of Odderon-exchange from scaling properties of elastic scattering at TeV energies. *Eur. Phys. J. C*, 81(2):180, 2021.
- [54] T. Csorgo and I. Szanyi. Observation of Odderon Effects at LHC energies – A Real Extended Bialas-Bzdak Model Study. 5 2020.
- [55] István Szanyi, Norbert Bence, and László Jenkovszky. New physics from TOTEM’s recent measurements of elastic and total cross sections. *J. Phys. G*, 46(5):055002, 2019.
- [56] Juan Martin Maldacena. The Large N limit of superconformal field theories and supergravity. *Adv. Theor. Math. Phys.*, 2:231–252, 1998.
- [57] S. S. Gubser, Igor R. Klebanov, and Alexander M. Polyakov. Gauge theory correlators from noncritical string theory. *Phys. Lett. B*, 428:105–114, 1998.
- [58] Edward Witten. Anti-de Sitter space and holography. *Adv. Theor. Math. Phys.*, 2:253–291, 1998.

- [59] Ofer Aharony, Steven S. Gubser, Juan Martin Maldacena, Hirosi Ooguri, and Yaron Oz. Large N field theories, string theory and gravity. *Phys. Rept.*, 323:183–386, 2000.
- [60] Ofer Aharony. The NonAdS / nonCFT correspondence, or three different paths to QCD. In *NATO Advanced Study Institute and EC Summer School on Progress in String, Field and Particle Theory*, 12 2002.
- [61] A. Zaffaroni. RTN lectures on the non AdS / non CFT correspondence. *PoS*, RTN2005:005, 2005.
- [62] Johanna Erdmenger, Nick Evans, Ingo Kirsch, and Ed Threlfall. Mesons in Gauge/Gravity Duals - A Review. *Eur. Phys. J. A*, 35:81–133, 2008.
- [63] P. Kovtun, Dan T. Son, and Andrei O. Starinets. Viscosity in strongly interacting quantum field theories from black hole physics. *Phys. Rev. Lett.*, 94:111601, 2005.
- [64] Joshua Erlich, Emanuel Katz, Dam T. Son, and Mikhail A. Stephanov. QCD and a holographic model of hadrons. *Phys. Rev. Lett.*, 95:261602, 2005.
- [65] Andreas Karch, Emanuel Katz, Dam T. Son, and Mikhail A. Stephanov. Linear confinement and AdS/QCD. *Phys. Rev. D*, 74:015005, 2006.
- [66] Tadakatsu Sakai and Shigeki Sugimoto. Low energy hadron physics in holographic QCD. *Prog. Theor. Phys.*, 113:843–882, 2005.
- [67] Tadakatsu Sakai and Shigeki Sugimoto. More on a holographic dual of QCD. *Prog. Theor. Phys.*, 114:1083–1118, 2005.
- [68] Guy F. de Teramond and Stanley J. Brodsky. Hadronic spectrum of a holographic dual of QCD. *Phys. Rev. Lett.*, 94:201601, 2005.
- [69] Leandro Da Rold and Alex Pomarol. Chiral symmetry breaking from five dimensional spaces. *Nucl. Phys. B*, 721:79–97, 2005.
- [70] Kazuo Ghoroku, Nobuhito Maru, Motoi Tachibana, and Masanobu Yahiro. Holographic model for hadrons in deformed AdS(5) background. *Phys. Lett. B*, 633:602–606, 2006.
- [71] Oleg Andreev and Valentin I. Zakharov. Gluon Condensate, Wilson Loops and Gauge/String Duality. *Phys. Rev. D*, 76:047705, 2007.
- [72] Oleg Andreev and Valentin I. Zakharov. Heavy-quark potentials and AdS/QCD. *Phys. Rev. D*, 74:025023, 2006.
- [73] Martin Kruczenski, Leopoldo A. Pando Zayas, Jacob Sonnenschein, and Diana Vaman. Regge trajectories for mesons in the holographic dual of large-N(c) QCD. *JHEP*, 06:046, 2005.
- [74] Stanislav Kuperstein and Jacob Sonnenschein. Non-critical, near extremal AdS(6) background as a holographic laboratory of four dimensional YM theory. *JHEP*, 11:026, 2004.
- [75] Hilmar Forkel, Michael Beyer, and Tobias Frederico. Linear square-mass trajectories of radially and orbitally excited hadrons in holographic QCD. *JHEP*, 07:077, 2007.
- [76] Deog Ki Hong, Takeo Inami, and Ho-Ung Yee. Baryons in AdS/QCD. *Phys. Lett. B*, 646:165–171, 2007.
- [77] Kanabu Nawa, Hideo Suganuma, and Toru Kojo. Baryons in holographic QCD. *Phys. Rev. D*, 75:086003, 2007.

- [78] Deog Ki Hong, Mannque Rho, Ho-Ung Yee, and Piljin Yi. Chiral Dynamics of Baryons from String Theory. *Phys. Rev. D*, 76:061901, 2007.
- [79] Csaba Csaki, Hiroshi Ooguri, Yaron Oz, and John Terning. Glueball mass spectrum from supergravity. *JHEP*, 01:017, 1999.
- [80] Robert de Mello Koch, Antal Jevicki, Mihail Mihailescu, and Joao P. Nunes. Evaluation of glueball masses from supergravity. *Phys. Rev. D*, 58:105009, 1998.
- [81] M. Zyskin. A Note on the glueball mass spectrum. *Phys. Lett. B*, 439:373–381, 1998.
- [82] Joseph A. Minahan. Glueball mass spectra and other issues for supergravity duals of QCD models. *JHEP*, 01:020, 1999.
- [83] Csaba Csaki, Yaron Oz, Jorge Russo, and John Terning. Large N QCD from rotating branes. *Phys. Rev. D*, 59:065012, 1999.
- [84] Csaba Csaki and John Terning. Glueball mass spectrum from supergravity. *AIP Conf. Proc.*, 494(1):321–328, 1999.
- [85] Richard C. Brower, Samir D. Mathur, and Chung-I Tan. Glueball spectrum for QCD from AdS supergravity duality. *Nucl. Phys. B*, 587:249–276, 2000.
- [86] Henrique Boschi-Filho and Nelson R. F. Braga. Gauge / string duality and scalar glueball mass ratios. *JHEP*, 05:009, 2003.
- [87] Henrique Boschi-Filho and Nelson R. F. Braga. QCD / string holographic mapping and glueball mass spectrum. *Eur. Phys. J. C*, 32:529–533, 2004.
- [88] Riccardo Areda, David E. Crooks, Nick J. Evans, and Michela Petrini. Confinement, glueballs and strings from deformed AdS. *JHEP*, 05:065, 2004.
- [89] Henrique Boschi-Filho, Nelson R. F. Braga, and Hector L. Carrion. Glueball Regge trajectories from gauge/string duality and the Pomeron. *Phys. Rev. D*, 73:047901, 2006.
- [90] P. Colangelo, F. De Fazio, F. Jugeau, and S. Nicotri. On the light glueball spectrum in a holographic description of QCD. *Phys. Lett. B*, 652:73–78, 2007.
- [91] Hilmar Forkel. Holographic glueball structure. *Phys. Rev. D*, 78:025001, 2008.
- [92] Eduardo Folco Capossoli and Henrique Boschi-Filho. Odd spin glueball masses and the Odderon Regge trajectories from the holographic hardwall model. *Phys. Rev. D*, 88(2):026010, 2013.
- [93] L. Bellantuono, P. Colangelo, and F. Giannuzzi. Holographic Oddballs. *JHEP*, 10:137, 2015.
- [94] Eduardo Folco Capossoli and Henrique Boschi-Filho. Glueball spectra and Regge trajectories from a modified holographic softwall model. *Phys. Lett. B*, 753:419–423, 2016.
- [95] Eduardo Folco Capossoli, Danning Li, and Henrique Boschi-Filho. Pomeron and Odderon Regge Trajectories from a Dynamical Holographic Model. *Phys. Lett. B*, 760:101–105, 2016.
- [96] Eduardo Folco Capossoli, Danning Li, and Henrique Boschi-Filho. Dynamical corrections to the anomalous holographic soft-wall model: the pomeron and the odderon. *Eur. Phys. J. C*, 76(6):320, 2016.
- [97] Diego M. Rodrigues, Eduardo Folco Capossoli, and Henrique Boschi-Filho. Twist Two Operator Approach for Even Spin Glueball Masses and Pomeron Regge Trajectory from the Hardwall Model. *Phys. Rev. D*, 95(7):076011, 2017.

- [98] Diego M. Rodrigues, Eduardo Folco Capossoli, and Henrique Boschi-Filho. Scalar and higher even spin glueball masses from an anomalous modified holographic model. *EPL*, 122(2):21001, 2018.
- [99] Eduardo Folco Capossoli, Miguel Angel Martín Contreras, Danning Li, Alfredo Vega, and Henrique Boschi-Filho. Hadronic spectra from deformed AdS backgrounds. *Chin. Phys. C*, 44(6):064104, 2020.
- [100] Daniel Elander. Glueball Spectra of SQCD-like Theories. *JHEP*, 03:114, 2010.
- [101] Daniel Elander and Maurizio Piai. Light scalars from a compact fifth dimension. *JHEP*, 01:026, 2011.
- [102] Massimo Bianchi, Maurizio Prisco, and Wolfgang Mueck. New results on holographic three point functions. *JHEP*, 11:052, 2003.
- [103] Marcus Berg, Michael Haack, and Wolfgang Mueck. Bulk dynamics in confining gauge theories. *Nucl. Phys. B*, 736:82–132, 2006.
- [104] Marcus Berg, Michael Haack, and Wolfgang Mueck. Glueballs vs. Gluinoballs: Fluctuation Spectra in Non-AdS/Non-CFT. *Nucl. Phys. B*, 789:1–44, 2008.
- [105] Daniel Elander and Maurizio Piai. On the glueball spectrum of walking backgrounds from wrapped-D5 gravity duals. *Nucl. Phys. B*, 871:164–180, 2013.
- [106] Daniel Elander and Maurizio Piai. Calculable mass hierarchies and a light dilaton from gravity duals. *Phys. Lett. B*, 772:110–114, 2017.
- [107] Daniel Elander and Maurizio Piai. Glueballs on the Baryonic Branch of Klebanov-Strassler: dimensional deconstruction and a light scalar particle. *JHEP*, 06:003, 2017.
- [108] Daniel Elander, Antón F. Faedo, David Mateos, David Pravos, and Javier G. Subils. Mass spectrum of gapped, non-confining theories with multi-scale dynamics. *JHEP*, 05:175, 2019.
- [109] Daniel Elander, Maurizio Piai, and John Roughley. Holographic glueballs from the circle reduction of Romans supergravity. *JHEP*, 02:101, 2019.
- [110] Daniel Elander, Maurizio Piai, and John Roughley. Probing the holographic dilaton. *JHEP*, 06:177, 2020. [Erratum: *JHEP* 12, 109 (2020)].
- [111] Daniel Elander, Maurizio Piai, and John Roughley. Dilatonic states near holographic phase transitions. *Phys. Rev. D*, 103:106018, 2021.
- [112] Daniel Elander, Michele Frigerio, Marc Knecht, and Jean-Loïc Kneur. Holographic models of composite Higgs in the Veneziano limit. Part I. Bosonic sector. *JHEP*, 03:182, 2021.
- [113] Daniel Elander, Maurizio Piai, and John Roughley. Light dilaton in a metastable vacuum. *Phys. Rev. D*, 103(4):046009, 2021.
- [114] Daniel Elander, Maurizio Piai, and John Roughley. The Coulomb branch of N=4 SYM and dilatonic scions in supergravity. 3 2021.
- [115] Koji Hashimoto, Chung-I Tan, and Seiji Terashima. Glueball decay in holographic QCD. *Phys. Rev. D*, 77:086001, 2008.
- [116] Frederic Brünner, Denis Parganlija, and Anton Rebhan. Glueball Decay Rates in the Witten-Sakai-Sugimoto Model. *Phys. Rev. D*, 91(10):106002, 2015. [Erratum: *Phys.Rev.D* 93, 109903 (2016)].

- [117] Frederic Br  nner and Anton Rebhan. Nonchiral enhancement of scalar glueball decay in the Witten-Sakai-Sugimoto model. *Phys. Rev. Lett.*, 115(13):131601, 2015.
- [118] Danning Li, Mei Huang, and Qi-Shu Yan. A dynamical soft-wall holographic QCD model for chiral symmetry breaking and linear confinement. *Eur. Phys. J. C*, 73:2615, 2013.
- [119] Danning Li and Mei Huang. Dynamical holographic QCD model for glueball and light meson spectra. *JHEP*, 11:088, 2013.
- [120] Mei Huang and Danning Li. Dynamical holographic QCD model: resembling renormalization group from ultraviolet to infrared. *Springer Proc. Phys.*, 170:367–372, 2016.
- [121] Danning Li, Jinfeng Liao, and Mei Huang. Enhancement of jet quenching around phase transition: result from the dynamical holographic model. *Phys. Rev. D*, 89(12):126006, 2014.
- [122] Danning Li, Song He, and Mei Huang. Temperature dependent transport coefficients in a dynamical holographic QCD model. *JHEP*, 06:046, 2015.
- [123] Kaddour Chelabi, Zhen Fang, Mei Huang, Danning Li, and Yue-Liang Wu. Realization of chiral symmetry breaking and restoration in holographic QCD. *Phys. Rev. D*, 93(10):101901, 2016.
- [124] Steven S. Gubser and Abhinav Nellore. Mimicking the QCD equation of state with a dual black hole. *Phys. Rev. D*, 78:086007, 2008.
- [125] Steven S. Gubser, Abhinav Nellore, Silviu S. Pufu, and Fabio D. Rocha. Thermodynamics and bulk viscosity of approximate black hole duals to finite temperature quantum chromodynamics. *Phys. Rev. Lett.*, 101:131601, 2008.
- [126] Oliver DeWolfe, Steven S. Gubser, and Christopher Rosen. A holographic critical point. *Phys. Rev. D*, 83:086005, 2011.
- [127] U. Gursoy and E. Kiritsis. Exploring improved holographic theories for QCD: Part I. *JHEP*, 02:032, 2008.
- [128] U. Gursoy, E. Kiritsis, and F. Nitti. Exploring improved holographic theories for QCD: Part II. *JHEP*, 02:019, 2008.
- [129] Umut Gursoy, Elias Kiritsis, Liuba Mazzanti, Georgios Michalogiorgakis, and Francesco Nitti. Improved Holographic QCD. *Lect. Notes Phys.*, 828:79–146, 2011.
- [130] Yi Yang and Pei-Hung Yuan. A Refined Holographic QCD Model and QCD Phase Structure. *JHEP*, 11:149, 2014.
- [131] David Dudal and Subhash Mahapatra. Thermal entropy of a quark-antiquark pair above and below deconfinement from a dynamical holographic QCD model. *Phys. Rev. D*, 96(12):126010, 2017.
- [132] Danning Li, Song He, Mei Huang, and Qi-Shu Yan. Thermodynamics of deformed AdS_5 model with a positive/negative quadratic correction in graviton-dilaton system. *JHEP*, 09:041, 2011.
- [133] Hermann Weyl and Henry L Brose. Raum–zeit–materie [space–time–matter]. *Lectures on General Relativity (in German)(Springer, Berlin, 1921)*, 1921.
- [134] H Weyl and J Ehlers. Space, time, matter: Lectures on general relativity. *Berlin, Germany: Springer*, 1993.

- [135] U. Gursoy, E. Kiritsis, L. Mazzanti, and F. Nitti. Holography and Thermodynamics of 5D Dilaton-gravity. *JHEP*, 05:033, 2009.
- [136] Yidian Chen and Mei Huang. Two-gluon and trigluon glueballs from dynamical holography QCD. *Chin. Phys. C*, 40(12):123101, 2016.
- [137] Renato Critelli, Jorge Noronha, Jacquelyn Noronha-Hostler, Israel Portillo, Claudia Ratti, and Romulo Rougemont. Critical point in the phase diagram of primordial quark-gluon matter from black hole physics. *Phys. Rev. D*, 96(9):096026, 2017.
- [138] Michele Caselle, Alessandro Nada, and Marco Panero. QCD thermodynamics from lattice calculations with nonequilibrium methods: The SU(3) equation of state. *Phys. Rev. D*, 98(5):054513, 2018.
- [139] Szabolcs Borsanyi, Zoltan Fodor, Christian Hoelbling, Sandor D. Katz, Stefan Krieg, and Kalman K. Szabo. Full result for the QCD equation of state with 2+1 flavors. *Phys. Lett. B*, 730:99–104, 2014.